

FRAMATOME ANP, Inc.

August 9, 2004
NRC:04:027

Document Control Desk
U.S. Nuclear Regulatory Commission
Washington, D.C. 20555-0001

Request for Review and Approval of EMF-2103(P) Revision 1, "Realistic Large Break LOCA Methodology for Pressurized Water Reactors"

Ref.: 1. EMF-2103(P)(A), "Realistic Large Break LOCA Methodology for Pressurized Water Reactors," April 2003.

Ref.: 2. Letter, James F. Mallay (Framatome ANP) to Document Control Desk (NRC), "Responses to a Request for Additional Information on EMF-2103(P) Revision 0, 'Realistic Large Break LOCA Methodology for Pressurized Water Reactors' (TAC No. MB2865)," NRC:02:062, December 20, 2002.

Framatome ANP requests the NRC's review and approval of a revision to the topical report EMF-2103(P)(A), "Realistic Large Break LOCA Methodology for Pressurized Water Reactors," Reference 1. The revision consists primarily of the addition of four appendices to the topical report. The appendices are presented in Attachment A to this letter.

The NRC requested further clarification of a number of issues after the approval of the Reference 1 topical report.

- Applicability of the Forslund-Rohsenow correlation to dispersed flow film boiling above T_{min}
- The impact of not having a rod-to-rod radiation model in S-RELAP5
- Containment modeling methodology
- Downcomer heat structure nodalization

The objective of this revision to EMF-2103 (P)(A), Reference 1, is to provide documentation to address these issues generically. The methodology approved in Reference 1 is not being modified by this revision.

Framatome ANP has identified a number of minor errors in the topical report subsequent to the issuance of the approved version. A set of change pages to the topical report to correct these errors is presented in Attachment B to this letter. The errors are as follows:

1. Page 4-93, the expression for the stored energy bias has a sign error
2. Page 4-144, Table 4.19 contains a number of small numerical errors

T007

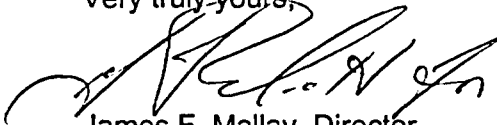
3. Page 5-5, the treatment of gadolinia bearing fuel was changed during the review process and the description of the treatment was not updated in the approved version of the report. The change in the treatment of gadolinia bearing fuel was described in Reference 2.
4. Page 5-7, two of the expressions defining the radial power profile have a sign error

A proprietary and non-proprietary version of this letter and its attachments are provided on the enclosed CDs. The additional appendices in Attachment A to this letter do not contain any proprietary information and thus only a non-proprietary version of Attachment A is provided.

Framatome ANP proposes to issue EMF-2301(P)(A) Revision 1 with the changes identified in Attachment A and B following NRC approval of these changes. The table of contents for the report will be revised to reflect the new appendices. Framatome ANP requests that the NRC issue a safety evaluation approving the proposed changes to the topical report EMF-2103 by the end of the year 2004.

Framatome ANP considers some of the material contained in the enclosed documents to be proprietary. As required by 10 CFR 2.390(b), an affidavit is enclosed to support the withholding of the information from public disclosure.

Very truly yours,



James F. Mallay, Director
Regulatory Affairs

Enclosures

cc: M. C. Honcharik
J. L. Uhle
Project 728

bcc: NRC:04:027

J. R. Biller
D. M. Brown
J. J. Cudlin
B. M. Dunn
G. F. Elliott
D. E. Garber
E. Giavedoni *EG*
D. A. Gottuso
K. R. Greene
G. E. Hanson
R. S. Heath
J. S. Holm *jsm*
J. A. Klingenfus
T. R. Lindquist
L. L. Losh
J. F. Mallay
R. P. Martin
F. A. Masseth
E. M. Miller
P. G. Newby
L. D. O'Dell
T. W. Patten
D. W. Pruitt
R. S. Reynolds
M. A. Schoppman
S. M. Sloan
J. R. Tandy
K. W. Turner
W. E. Van Scooter, Jr.
R. D. Williamson
J. A. Zwetolitz

AFFIDAVIT

STATE OF WASHINGTON)
) ss.
COUNTY OF BENTON)

1. My name is Jerald S. Holm. I am Manager, Product Licensing, for Framatome ANP ("FANP"), and as such I am authorized to execute this Affidavit.

2. I am familiar with the criteria applied by FANP to determine whether certain FANP information is proprietary. I am familiar with the policies established by FANP to ensure the proper application of these criteria.

3. I am familiar with the FANP information in the letter number NRC:04:027 and its attachments, dated August 2, 2004, and referred to herein as "Documents." Information contained in these Documents has been classified by FANP as proprietary in accordance with the policies established by FANP for the control and protection of proprietary and confidential information.

4. These Documents contain information of a proprietary and confidential nature and is of the type customarily held in confidence by FANP and not made available to the public. Based on my experience, I am aware that other companies regard information of the kind contained in these Documents as proprietary and confidential.

5. These Documents have been made available to the U.S. Nuclear Regulatory Commission in confidence with the request that the information contained in these Documents be withheld from public disclosure.

6. The following criteria are customarily applied by FANP to determine whether information should be classified as proprietary:

- (a) The information reveals details of FANP's research and development plans and programs or their results.
- (b) Use of the information by a competitor would permit the competitor to significantly reduce its expenditures, in time or resources, to design, produce, or market a similar product or service.
- (c) The information includes test data or analytical techniques concerning a process, methodology, or component, the application of which results in a competitive advantage for FANP.
- (d) The information reveals certain distinguishing aspects of a process, methodology, or component, the exclusive use of which provides a competitive advantage for FANP in product optimization or marketability.
- (e) The information is vital to a competitive advantage held by FANP, would be helpful to competitors to FANP, and would likely cause substantial harm to the competitive position of FANP.

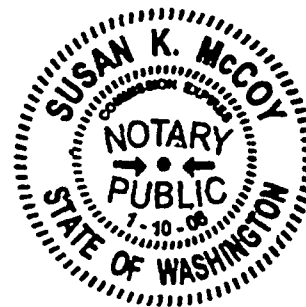
7. In accordance with FANP's policies governing the protection and control of information, proprietary information contained in these Documents have been made available, on a limited basis, to others outside FANP only as required and under suitable agreement providing for nondisclosure and limited use of the information.

8. FANP policy requires that proprietary information be kept in a secured file or area and distributed on a need-to-know basis.

9. The foregoing statements are true and correct to the best of my knowledge,
information, and belief.

Gerald S Holm

SUBSCRIBED before me this 22
day of August, 2004



Susan K McCoy

Susan K. McCoy
NOTARY PUBLIC, STATE OF WASHINGTON
MY COMMISSION EXPIRES: 1/10/08

Attachment A

Appendices G, H, J, I to EMF-2103, "Realistic Large Break LOCA
Methodology for Pressurized Water Reactors"

Contents

Appendix F	Applicability of Forslund-Rohsenow Correlation	F-1
F.1	Description of Forslund and Rohsenow's Work	F-1
F.2	Supplemental S-RELAP5 Benchmarks	F-4
F.2.1	Test Description	F-5
F.2.2	Calculation Results.....	F-6
F.3	Conclusions.....	F-18
F.4	References	F-18
Appendix G	Rod-to-Rod Radiation	G-1
G.1	Qualitative Assessment of Thermal Radiation for Best-Estimate Methodologies.....	G-1
G.2	Supplemental Quantification of the Impact of Thermal Radiation	G-3
G.1.2	17x17 Assembly Study.....	G-4
G.2.2	15x15 Assembly Study.....	G-6
G.2.3	Minimum Separation of Powers Study	G-9
G.3	Conclusions.....	G-11
G.4	References.....	G-12
Appendix H	Containment Pressure	H-1
H.1	S-RELAP5 Containment Model History	H-1
H.2	Containment Model Characterization.....	H-2
H.2.1	Passive Heat Sinks – Uchida Model.....	H-3
H.2.2	Break Flow	H-6
H.2.3	Initial Containment Pressure and Temperature.....	H-6
H.2.4	Inherent Conservatisms	H-6
H.2.5	Choice of Nominal Versus Conservative Values	H-8
H.2.6	Drywell Versus Ice Condenser Containment Modeling and Uncertainty Treatment.....	H-11
H.3	Impact of Unmodeled Parameters	H-12
H.4	Conclusion	H-13
H.5	References.....	H-13
Appendix I	Downcomer Heat Structure Nodalization Technical Basis.....	I-1

Appendix F Applicability of Forslund-Rohsenow Correlation

The S-RELAP5 code employs the Forslund-Rohsenow correlation for the purpose of predicting the convective wall-to-liquid-droplet heat transfer component of disperse flow film boiling (DFFB). The heat transfer mechanisms modeled by S-RELAP5 to describe DFFB are wall-to-vapor convection, wall-to-liquid droplet convection, thermal radiation to liquid droplets, thermal radiation to vapor, and convection between phases. References 1 and 2 detail the models used for simulating these processes and how these models are applied in S-RELAP5. During DFFB, the primary heat transfer mechanism is wall-to-vapor convection.

F.1 Description of Forslund and Rohsenow's Work

The Forslund-Rohsenow correlation was developed based on the work performed in Reference 3 and reported in Reference 4. The form of the Forslund-Rohsenow correlation was modeled on work done by Baumeister (Reference 5). The Baumeister work in turn was based on the Bromley correlation for DFFB described in Reference 6. For this reason the formulation of the Forslund-Rohsenow correlation appears similar to that of the Bromley correlation.

Forslund and Rohsenow state the purpose of their work to be (Reference 3):

- "The present work extends Laverty's work by including the effects of droplet breakup, "Leidenfrost" heat transfer from the wall to the droplets, and modifies the drag coefficients for accelerating droplets."
- "Concern here is with the dispersed-flow-film-boiling region where heat is transferred from the wall to a possibly superheated vapor and from this vapor to liquid droplets. Superimposed on this two-step process is an additional amount of heat that transferred from the tube wall directly to the liquid droplets, a kind of Leidenfrost effect."

Forslund's experiment was designed to operate above the Leidenfrost temperature so that film boiling would exist. The test apparatus consisted of a heated tube that was injected with saturated nitrogen at 25 psia and -312°F. Tube lengths of 4 and 8 feet with diameters of 0.228, 0.323, and 0.462 inches were included in the tests. The wall temperature data were taken at different powers and inlet flows. The mass velocity was varied from 70,000 to 190,000 lbm/hr/ft² and the heat flux was varied from 5,000 to 25,000 Btu/hr/ft² in the experiment.

Forslund observed that stable film boiling was consistently obtained in the test apparatus by first applying heater power until the test section was above the Leidenfrost temperature. Once the

desired test section temperature was reached, nitrogen flow was initiated. This resulted in the full length of the test section being in film boiling. Figure F.1, from Reference 4, shows the measured data for both the 4-ft and 8-ft lengths in the 0.323 inch diameter tubes at a nitrogen flow rate of 70,000 lbm/hr/ft². Annotations appear in the figure identifying the test T_{sat} and T_{min} . The data shown in Figure F.1 cover a heat flux range from 5,000 to 20,000 Btu/hr/ft². The measured wall temperatures are shown to range from 400 to 1,200 R.

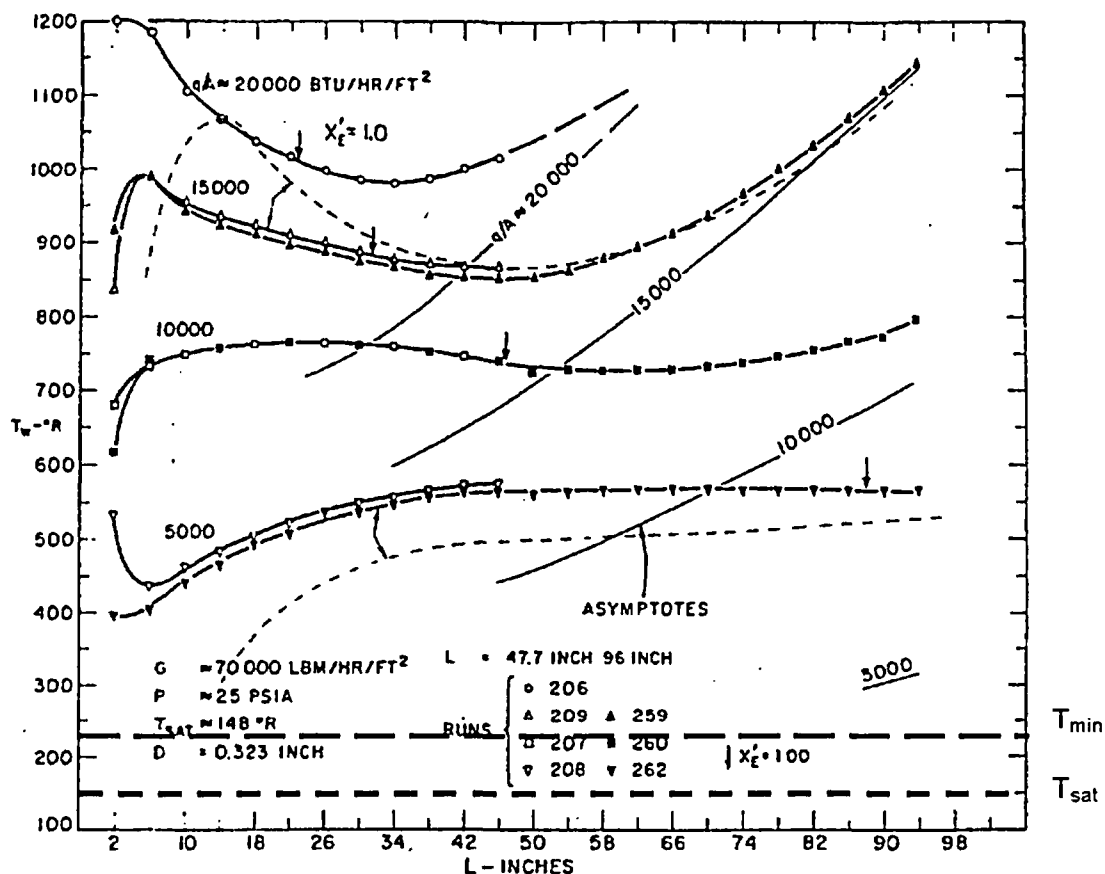


Figure F.1 Tube Wall Temperatures Profiles

In Reference 7, Hynek measured the minimum heat flux for nitrogen that would support film boiling. At the experimental conditions of 30 psia, a heat flux of 2,200 Btu/hr/ft² and a mass flux of 40,000 lbm/hr/ft², a T_{min} of 220 R was obtained. When this is compared to the wall temperature range measured in Forslund's experiment it is apparent that the data were obtained above T_{min} . Thus, the resulting Forslund-Rohsenow correlation was developed based on data

taken above T_{min} and consequently is applicable above T_{min} . This is consistent with the correlation application in the S-RELAP5 code.

To further substantiate the application of the Forslund-Rohsenow correlation above T_{min} , a number of publications were reviewed, References 8 through 15. With the exception of Reference 14, all the references consider the Forslund-Rohsenow correlation appropriate for application in DFFB above T_{min} . Reference 14 acknowledges that the Forslund-Rohsenow correlation is based on Baumeister's work (Reference 5) and notes the similarity to Bromley's equation. No justification is provided in Reference 14 for the use of the correlation below T_{min} other than to indicate that its use "does not have a critical influence on the overall analysis."

Reference 15 recognizes the work of Forslund-Rohsenow as one of

Two basic approaches have been taken to estimate the heat flux to droplets entering the thermal boundary layer but which do not touch the wall. ... Forslund and Rohsenow (1966), Hynek et al. (1966) and Course and Roberts (1974) have assumed the heat transfer coefficient to a single droplet in the spheroidal state condition on a flat heated plate and then multiplied this by the number of droplets approaching the surface per unit time per unit area.

The authors describe the Forslund-Rohsenow correlation as a "dry" collision/contact model: indicating that a dry contact model addresses the "heat transfer from the surface to liquid droplets which enter the thermal boundary layer but which do not 'wet' the surface", i.e., they do not actually contact the wall. This is consistent with Forslund's observation of droplets approaching but not touching the wall and is consistent with the experimental data being taken above T_{min} .

As a statistics-based methodology, Framatome ANP's (FANP) RLBLOCA methodology applies a code bias related to DFFB heat transfer. The code bias for DFFB was determined to be 1.75, which means that heat transfer predicted by the modeled heat transfer correlations must be multiplied by 1.75 for best-estimate agreement with test data. The form of the Forslund-Rohsenow correlation incorporates a similar constant multiplier, K, which was evaluated by a number of investigators to be, by convention, a parameter dependent on the chosen working fluid. The value of K derived by Forslund and Rohsenow for their experiments with nitrogen flowing through tubes was 0.2, which is used in the correlation as it is applied in the S-RELAP5 code. This is significantly lower than the constant of 1.1 obtained by Baumeister for water droplets on a flat plate (Reference 5). Reference 16 indicates that the value of K could

range from 0.2 to 2.0 for various fluids and References 17 and 18 indicate that the most appropriate value of K is 0.4 for water droplets in tubes. The form of the Forslund-Rohsenow equation, as evaluated for applications using water, remains conservative relative to the literature recommendations after the inclusion of the 1.75 code bias multiplier. Specifically, the 1.75 bias, when multiplied times the K of 0.2 used in S-RELAP5, provides an overall K of 0.35 ($1.75 \times 0.2 = 0.35$) and the correlation remains conservative relative to the best-estimate value, recommended in the literature, of 0.4.

F.2 Supplemental S-RELAP5 Benchmarks

Extensive assessment and uncertainty analysis of the ability of S-RELAP5 to predict film boiling heat transfer in rod bundles is documented in References 19 and 20. Table F.1 summarizes the key results from the particular tests originally used to develop and assess FANP's RLBLOCA methodology. Consistent with the conventional best-estimate methodology philosophy, this RLBLOCA methodology explicitly applies code bias and uncertainty multipliers in the development of the code input necessary to quantify code results with a statistical statement of coverage and confidence. DFFB heat transfer is one of the explicitly treated uncertainty parameters. The test suite used to derive the code bias and uncertainty for DFFB heat transfer included seven tests from the FLECHT-SEASET program and nine tests from the THTF program. The code bias determined from the uncertainty analysis was validated against both separate- and integral-effects test programs including LOFT, Semiscale, and CCTF. Validation of uncertainty was made by apportioning out a random 20 percent of the data from the FLECHT-SEASET and THTF programs as a "Validation Set". Comparisons were also made against two tests from the FLECHT-Skewed program.

Table F.1 FLECHT Assessment Tests With Key Results

Run No.	Peak Measured PCT (°F)	Average Measured PCT (°F) ^a
13609	1,761	1,747
13914	1,680	1,648
31203	1,879	1,809
31302	1,696	1,598
31504	2,101	2,017
31701	1,694	1,593
31805	2,239	2,172
32013	2,100	2,037
34209	2,114	2,060

F.2.1 Test Description

To supplement the previous work, two additional FLECHT-SEASET tests and one additional FLECHT-Skewed test were benchmarked. These tests were identified based on their characteristic of exhibiting clad temperature conditions near the regulatory limit of 2,200 °F. Table F.2 summarizes the relevant test information.

Table F.2 Supplemental Assessment Tests With Key Results

Run No.	Peak Measured PCT (°F)	Average Measured PCT (°F) ^a
15606	2,191	2,166
32333	2,076	1,987
34420	2,205	2,151

Input models for the supplemental assessment calculations were built following the same nodalization and modeling strategy employed for previous FLECHT assessments and analysis.

Calculations were performed with both the unbiased code and with the code bias multiplier (1.75). While the RLBLOCA methodology applies code biases for production analyses, for reflood tests such as FLECHT-SEASET and FLECHT-Skewed, the unbiased code results

^a Based on the average PCT of instrumented rods in the "hot region" (> 2 rows from assembly wall).

approximate a one-sided uncertainty coverage of approximately 97 percent (+2 standard deviations). The unbiased code result aligns with the highest measured temperature, while the biased code result aligns with the average measured temperature. For comparison purposes the average measured temperature is conservatively calculated as the average of PCT values for the instrumented rods in the "hot region"; that is, at least two rows away from the assembly wall (only these rods were used in the evaluation of code uncertainty).

The key parameters for comparison between the S-RELAP5 simulations and test results were established in prior assessments (Reference 1 and 19). These are maximum clad temperature versus elevation, rod surface temperature at various elevations versus time, steam temperature at an elevation versus time, heat transfer coefficient at an elevation versus time, and bundle mass inventory versus time. Additionally for these assessments, calculated heat transfer coefficients versus void fraction from each test case and by particular heat transfer mechanism are presented.

F.2.2 Calculation Results

For each test modeled, two assessment calculations were performed: one with the unbiased code and one applying the 1.75 DFFB code bias. The calculated PCT (without bias) should be compared against the peak measured PCT and the calculated PCT with bias (intended to be a best-estimate calculation) should be compared against the average measured PCT.

The comparisons for the previous assessment cases are shown in Table F.3. The calculated PCT is larger than the peak measured PCT in seven of the nine cases. This indicates that the use of the correlation without the bias is significantly conservative. The calculated PCT with bias is greater than the average measured PCT in six of the nine cases. This indicates that while the use of the bias brings the calculated and measured temperatures closer together, the correlation remains conservative even after the application of the bias.

The comparisons for the new assessment cases are shown in Table F.4. The calculated PCT (without bias) is larger than the peak measured PCT in all three of the new cases. The calculated PCT with bias is greater than the average measured PCT in all three of the new cases. The FLECHT-SEASET calculations using a bias of 1.75 for the DFFB regime show that the calculations bound the average measured PCT and are within 79°F of the hot rod PCT. The

FLECHT-Skewed calculation applying the 1.75 code bias significantly exceeds both the average measured and peak measured temperatures.

Table F.3 PCT Results From Data and Code Comparisons – Previous Assessments

Run No.	Peak Measured PCT (°F)	Average Measured PCT (°F) ^a	Calculated PCT (°F)	Calculated PCT With Bias (°F)
13609	1,761	1,747	2,285	2,028
13914	1,680	1,648	2,134	1,925
31203	1,879	1,809	1,927	1,848
31302	1,696	1,598	1,705	1,684
31504	2,101	2,017	2,157	2,046
31701	1,694	1,593	1,624	1,602
31805	2,239	2,172	2,254	2,167
32013	2,100	2,037	2,080	2,032
34209	2,114	2,060	2,193	2,051

Table F.4 PCT Results From Data and Code Comparisons – New Assessments

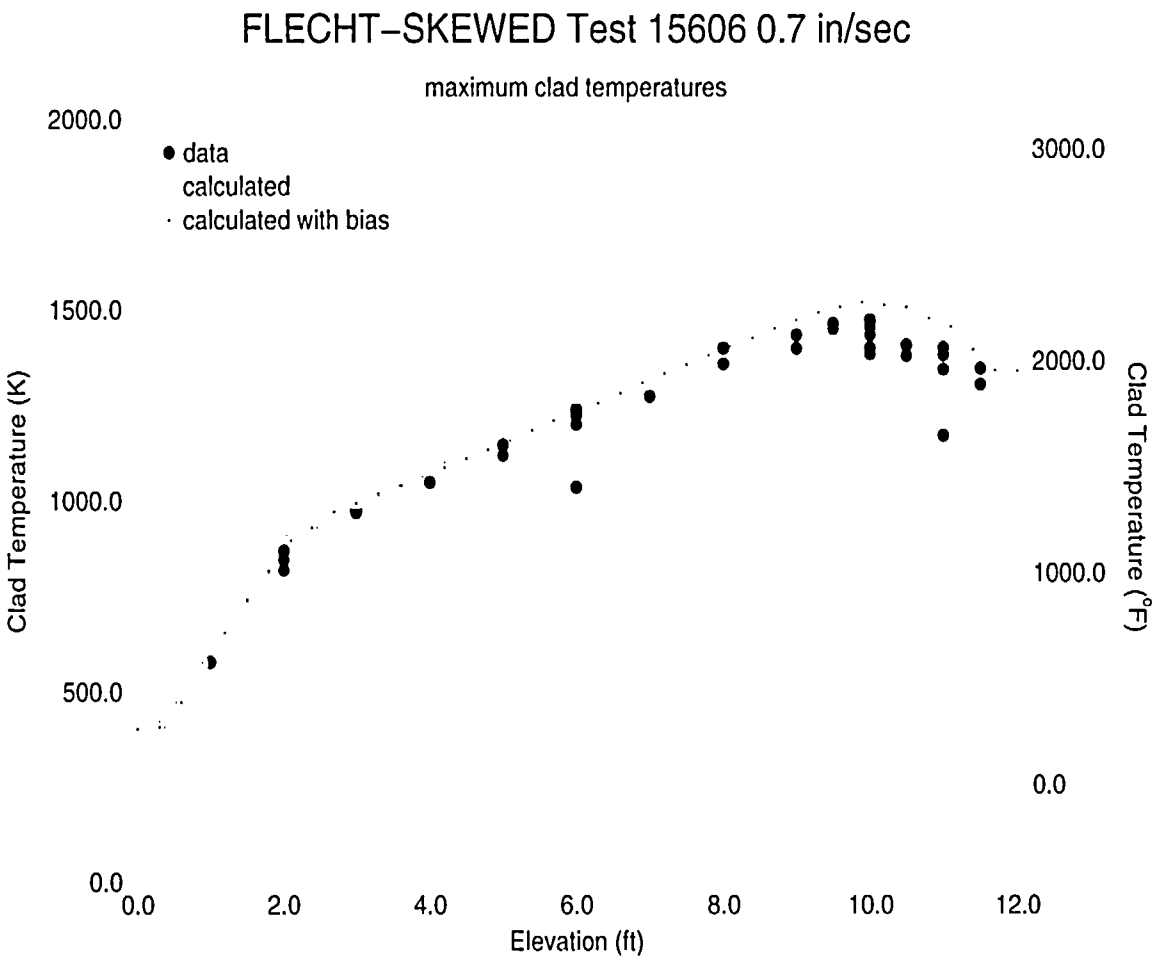
Run No.	Peak Measured PCT (°F)	Average Measured PCT (°F) ^a	Calculated PCT (°F)	Calculated PCT With Bias (°F)
15606	2,191	2,166	2,384	2,278
32333	2,076	1,987	2,126	1,997
34420	2,205	2,151	2,231	2,170

The comparisons between calculated clad temperatures and data are shown in Figures F.2 to F.4 for the new assessments. Those figures include the maximum measured and calculated clad temperatures as a function of test section (assembly) elevation. The data were taken from the published reports, References 20 and 21, in the form of tables summarizing the experimental results. The calculated temperatures were made with and without the RLBLOCA biases applied to the S-RELAP5 model. In each figure, the calculated temperatures are either greater than or equal to the measured temperatures at the measurement locations. After applying the biases, the calculated temperatures better predict the measured temperatures in the regions of the power peak. However, the biased calculated temperatures from Test 15606,

^a Based on the average PCT of instrumented rods in the "hot region" (> 2 rows from assembly wall).

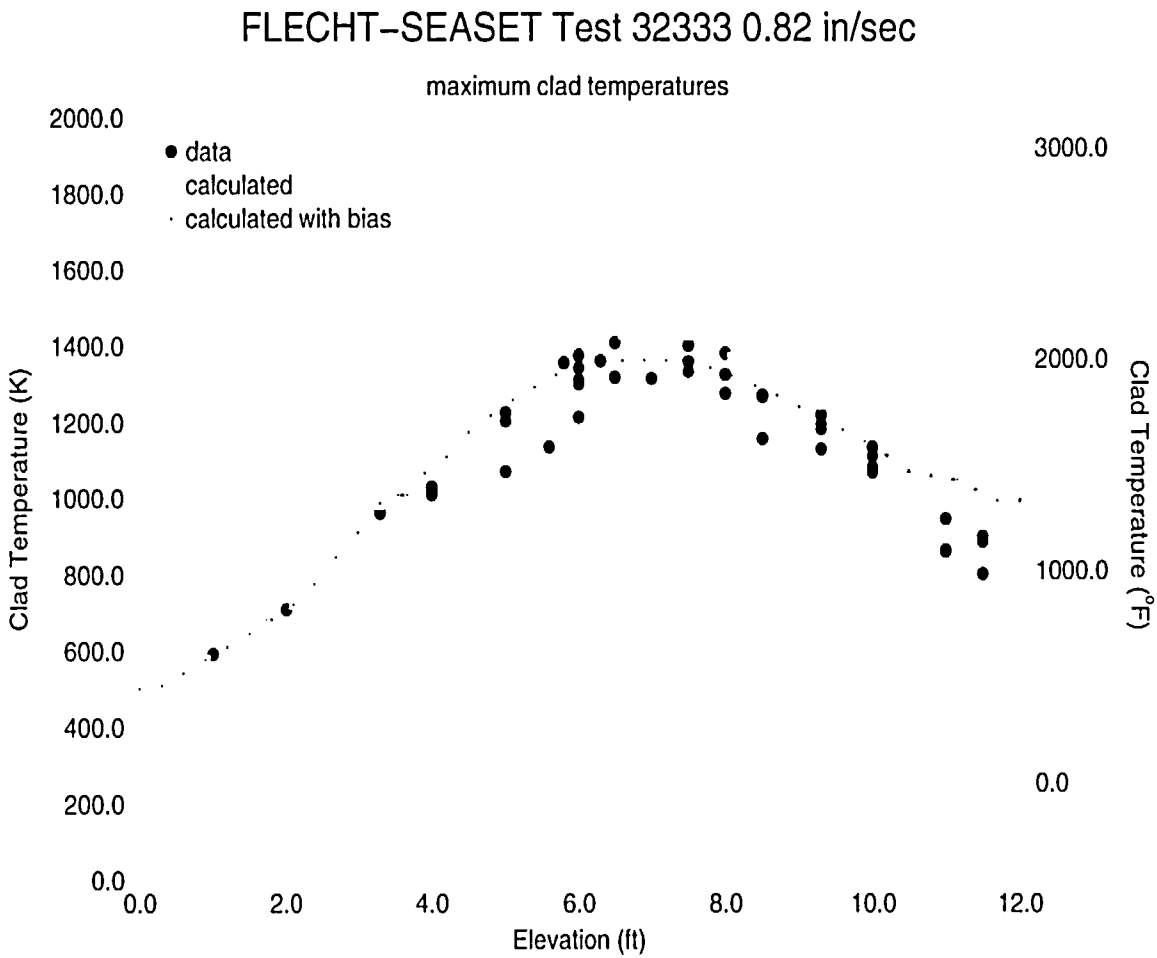
Figure F.2, tend to exceed the data throughout the test section while the biased calculated temperatures from Tests 32333 and 34420, shown in Figure F.3 and Figure F.4, respectively, lie within the data scatter.

S-RELAP5 uses the Forslund-Rohsenow correlation for convective heat transfer to liquid droplets in the DFFB heat transfer regime. Figures F.5, F.7, and F.9 show the effects of this correlation in relationship to the temperature turnaround (PCT). The S-RELAP5 heat transfer coefficients were extracted by heat transfer mechanism (e.g., convection to vapor, radiation to vapor, etc.) with respect to the PCT node void fraction from each of the tests for a period beginning at 10 seconds to the time of PCT for Tests 15606, 32333 and 34420. Figures F.6, F.8, and F.10 present this same information incorporating data from the total simulation time period. The legend indicates each of the symbols used for the four heat transfer coefficients plus their sum ("htc total").



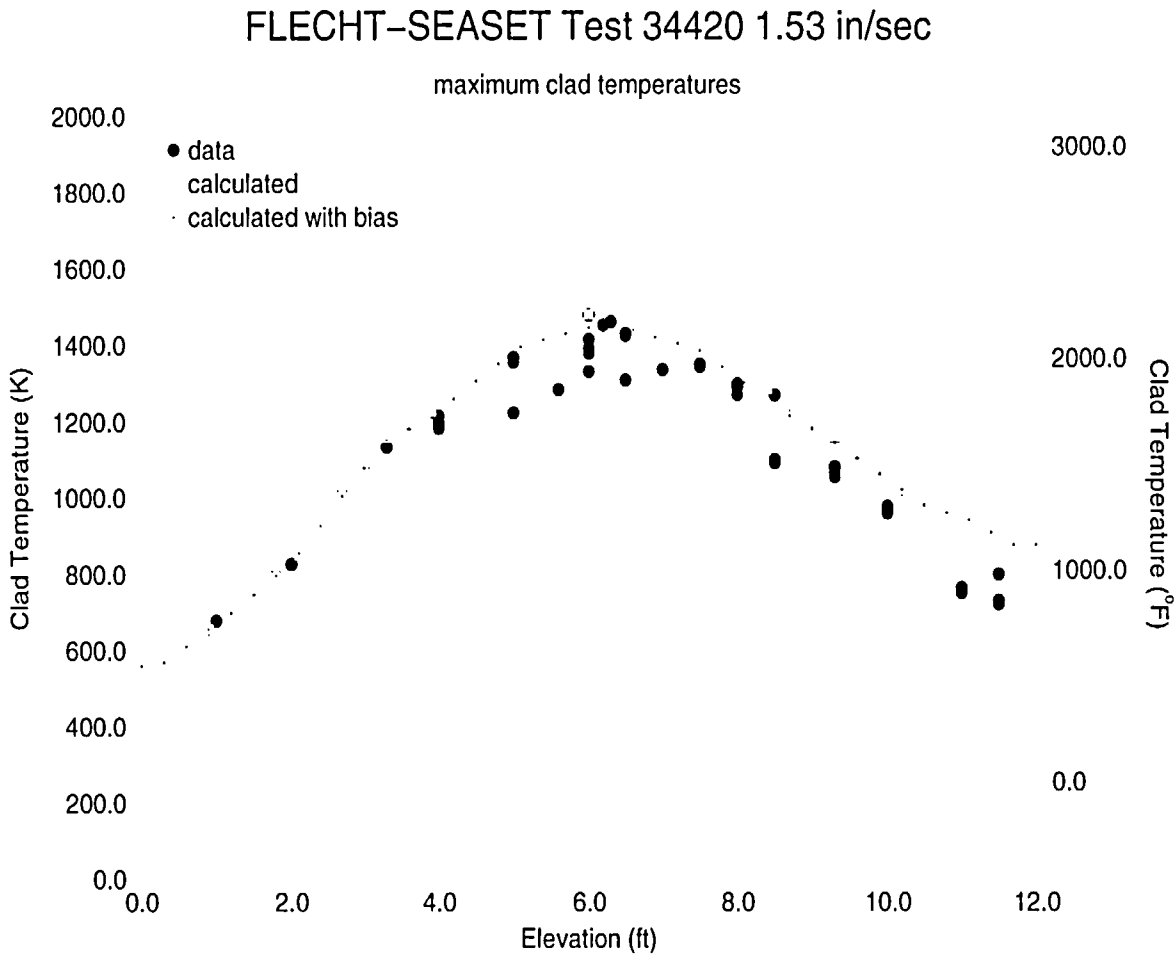
Framatome-ANP Proprietary

Figure F.2 Maximum Clad Temperature Comparison Between
S-RELAP5 and Measured Data From FLECHT Test 15606



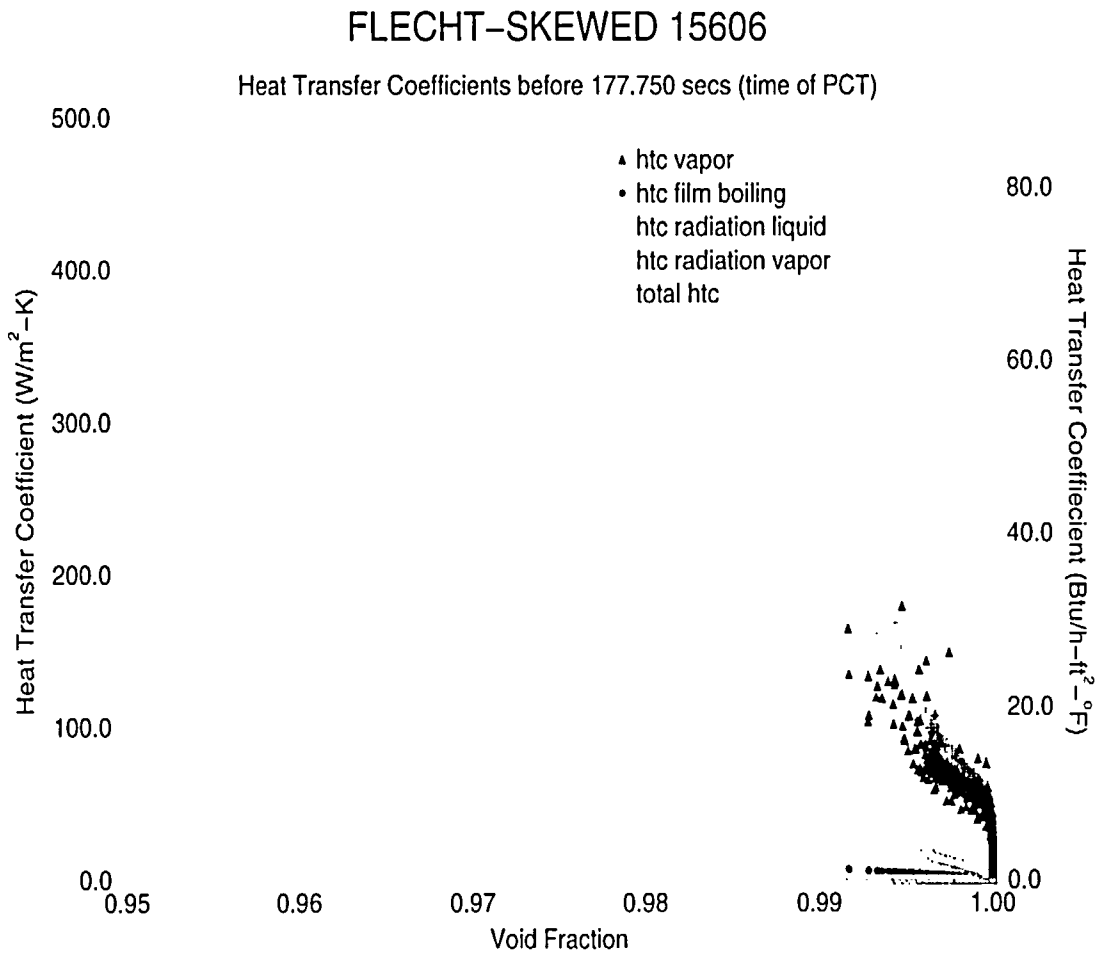
Framatome-ANP Proprietary

Figure F.3 Maximum Clad Temperature Comparison Between
S-RELAP5 and Measured Data From FLECHT Test 32333



Framatome-ANP Proprietary

Figure F.4 Maximum Clad Temperature Comparison Between
S-RELAP5 and Measured Data From FLECHT Test 34420



Framatome-ANP Proprietary

Figure F.5 S-RELAP5 Heat Transfer Coefficients From Test 15606 of
the PCT Node Prior to Time of PCT

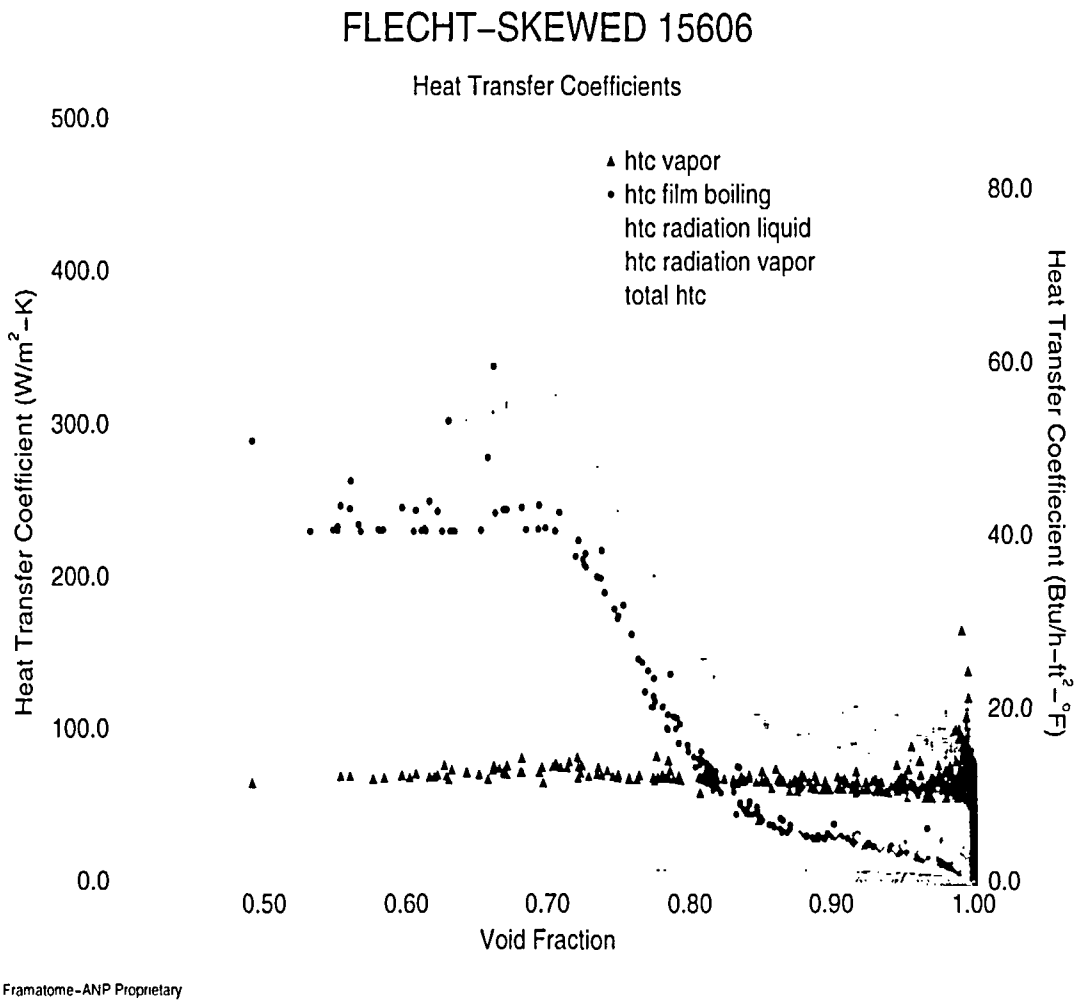


Figure F.6 S-RELAP5 Heat Transfer Coefficients From Test 15606 at
the PCT Node

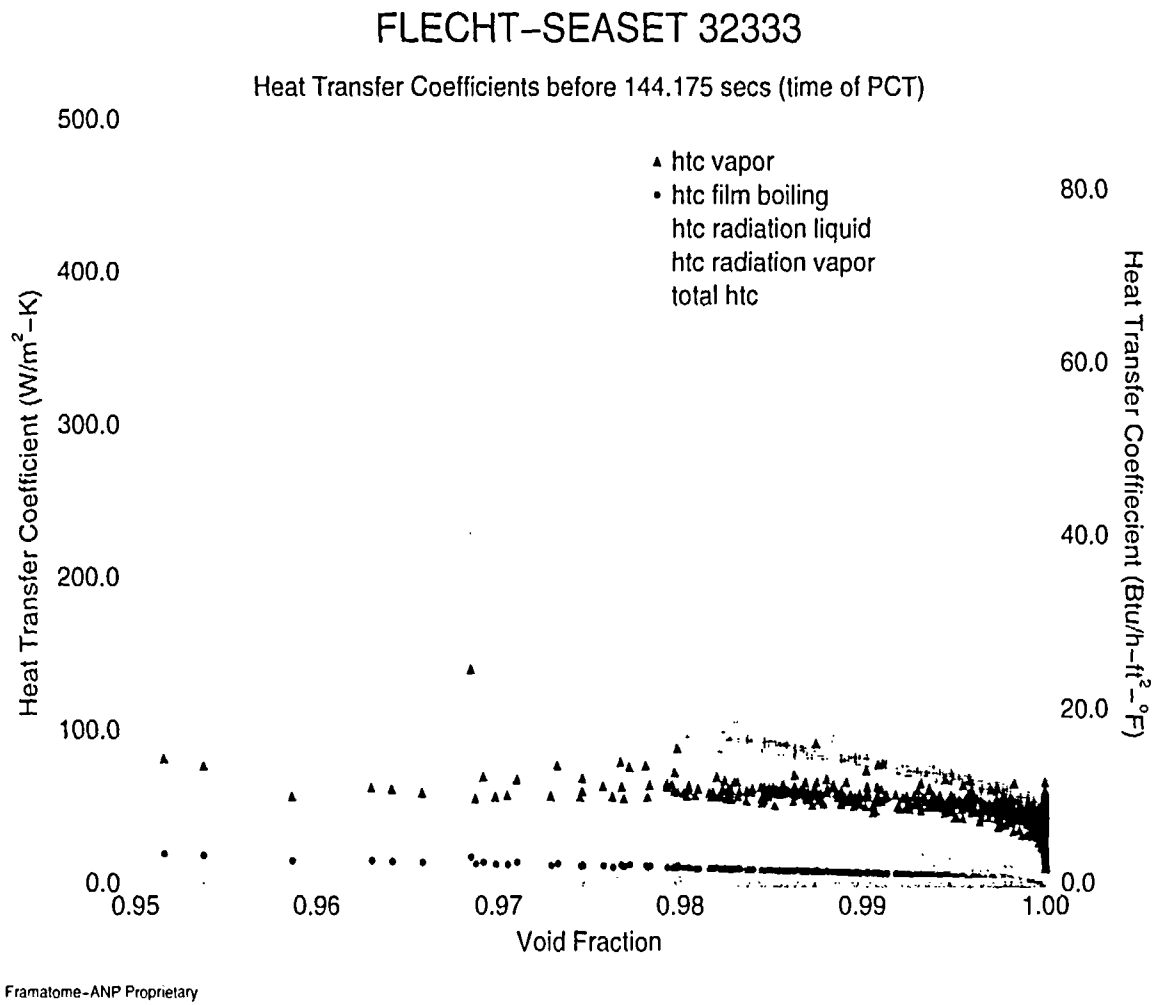
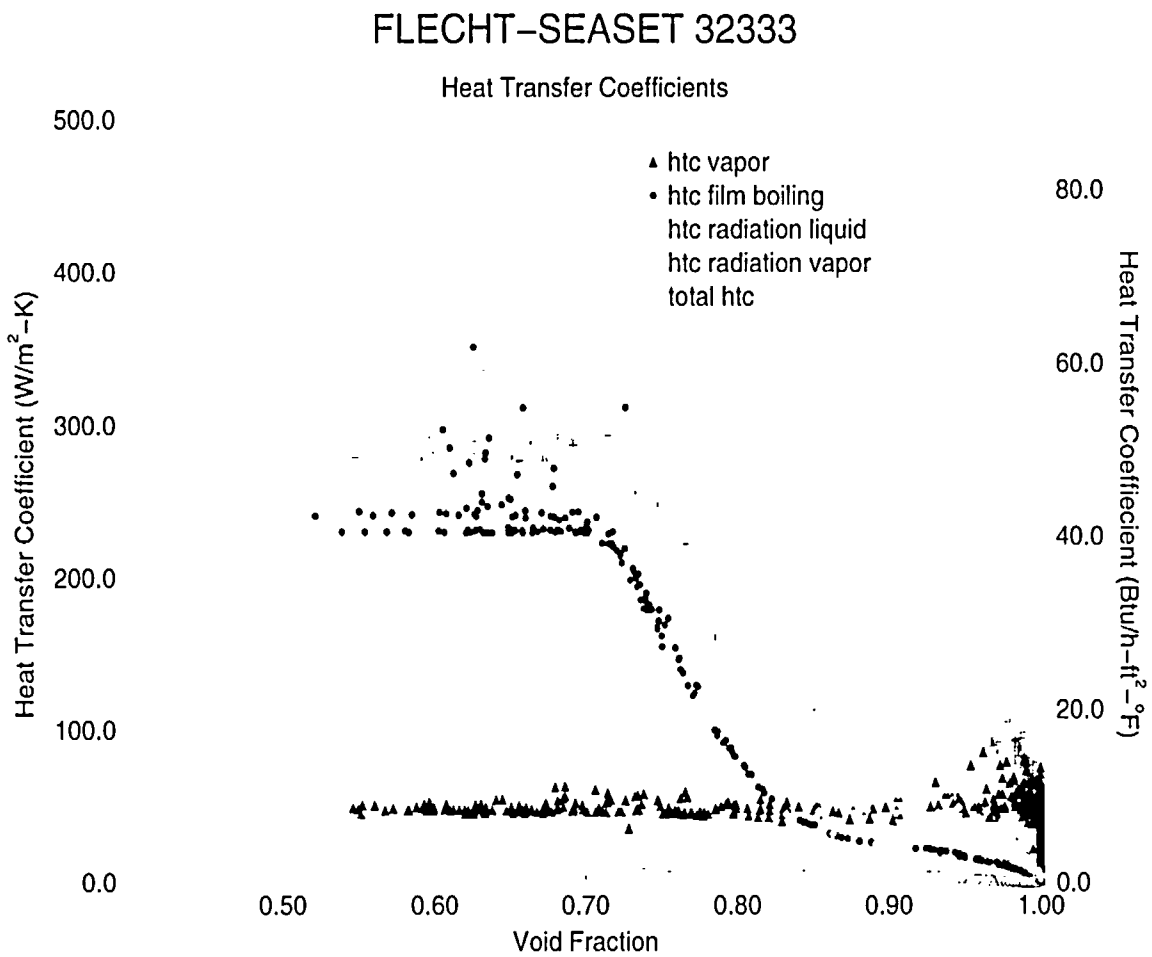
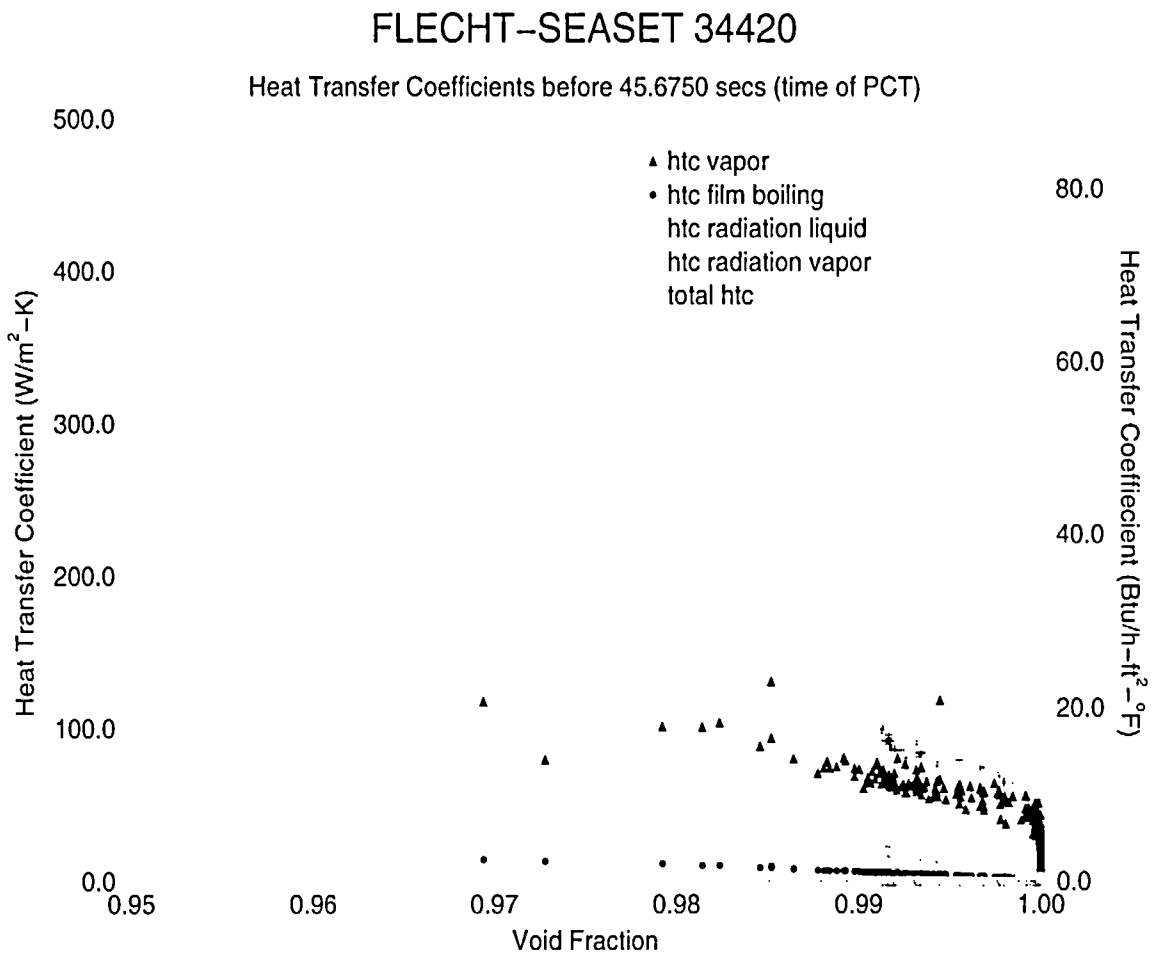


Figure F.7 S-RELAP5 Heat Transfer Coefficients From Test 32333 of
the PCT Node Prior to Time of PCT



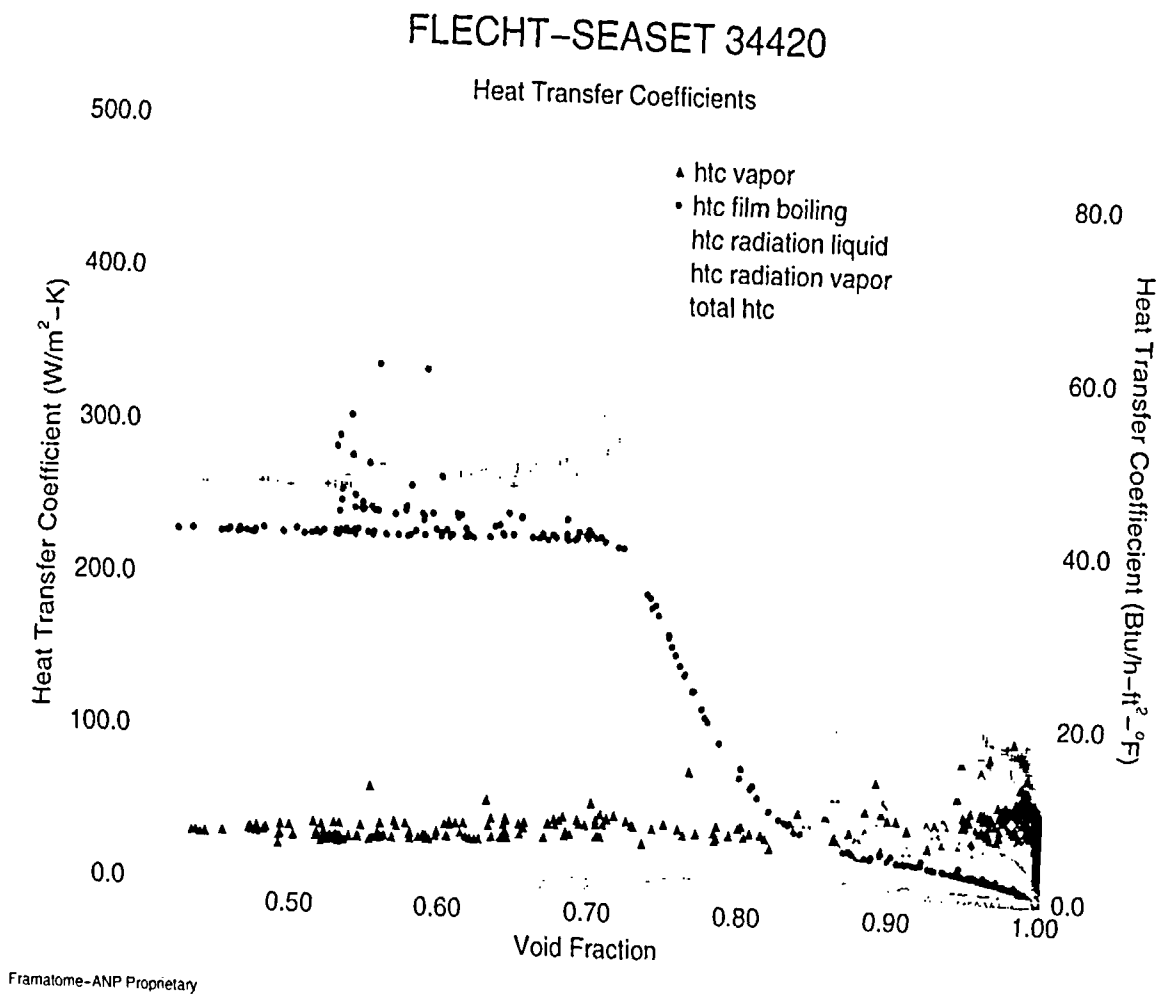
Framatome-ANP Proprietary

Figure F.8 S-RELAP5 Heat Transfer Coefficients From Test 32333
at the PCT Node



Framatome-ANP Proprietary

Figure F.9 S-RELAP5 Heat Transfer Coefficients From Test 34420 of
the PCT Node Prior to Time of PCT



**Figure F.10 S-RELAP5 Heat Transfer Coefficients From Test 34420
at the PCT Node**

F.3 Conclusions

The calculation results from the three supplemental assessment calculations and from the original nine assessments show that the S-RELAP5 code captures the best-estimate data trends by falling in the middle of the data or higher when applying the code bias. The calculation results from the unbiased code are generally higher than the measured data (representing the one-side 97 percent uncertainty coverage). In addition, the convective heat transfer from the wall to the liquid droplets, as modeled with the Forslund-Rohsenow correlation, represents only a small part of the total heat transfer at the time of PCT.

Framatome ANP's basis for using the Forslund-Rohsenow correlation is founded in the numerous literature citations indicating that the correlation is generally recognized as applicable as a "dry contact" model in dispersed flow film boiling above T_{min} . This previous work acknowledges that the conditions observed in Forslund's experiment supports application of the Forslund-Rohsenow correlation to dispersed flow film boiling above T_{min} . The code assessment results validate this assertion. Finally, the Forslund-Rohsenow correlation, as used in S-RELAP5, is based on the original experiment using nitrogen. This form results in roughly half the heat transfer expected when the working fluid is water. With the application of the 1.75 DFFB heat transfer code bias developed by comparing the S-RELAP5 code results to data, the form of the Forslund-Rohsenow correlation applied in the RLBLOCA methodology is consistent with respect to the form recommended for water in previously published work.

F.4 References

1. EMF-2103 (P)(A) Revision 0, *Realistic Large Break LOCA Methodology*, Siemens Power Corporation, April 2003.
2. EMF-2100 (P) Revision 4, *S-RELAP5 Models and Correlations Code Manual*, Framatome ANP, May 2001.
3. Technical Report No. 75312-44, *Thermal non-Equilibrium in Dispersed Flow Film Boiling in a Vertical Tube*, R. P. Forslund and W. M. Rohsenow, Department of Mechanical Engineering, Massachusetts Institute of Technology, November 1966.
4. R. P. Forslund and W. M. Rohsenow, *Dispersed Flow Film Boiling*, Journal of Heat Transfer, Transactions of the ASME, November 1968.
5. K. J. Baumeister, T. D. Hamill, and G. J. Schoessow, *A Generalized Correlation of Vaporization Time of Drops in Film Boiling on a Flat Plate*, US-AIChE No. 120, 3rd International Heat Transfer Conference and Exhibit, August 1966.

6. L. A. Bromley, *Heat Transfer in Stable Film Boiling*, Chemical Engineering Progress, Vol. 46, No. 5, 1950.
7. Technical Report No. 70586-63, *Forced-Convection, Dispersed-Flow Film Boiling*, S. J. Hynek, W. M. Rohsenow, and A. E. Bergles, Department of Mechanical Engineering, Massachusetts Institute of Technology, April 1969.
8. S. M. Bajorek, and M. Y. Young, *Direct-Contact Heat Transfer Model for Dispersed-Flow Film Boiling*, Nuclear Technology, Vol. 132, December 2000.
9. M. Andreani and G. Yadigaroglu, *Prediction Methods for Dispersed Flow Film Boiling*, International Journal Multiphase Flow, Vol. 20, Supplement, 1994.
10. G. Yadigaroglu, et. al., *Modeling of Reflooding*, Nuclear Engineering and Design 145, 1993.
11. NUREG/IA-0042, *Dispersed Flow Film Boiling*, M. Andreani and G. Yadigaroglu, Paul Scherrer Institute, August 1992.
12. A. F. Varone, Jr. and W. M. Rohsenow, *Post Dryout heat Transfer Prediction*, Nuclear Engineering and Design 95, 1986.
13. G. L. Yoder, Jr. and W. M. Rohsenow, *A Solution for Dispersed Flow Heat Transfer Using Equilibrium Fluid Conditions*, Journal of Heat Transfer, Transactions of the ASME, February 1983.
14. NUREG-0106, Vols. I and II, NRC-2,4, *Reflood Heat Transfer in a Light Water Reactor*, W. L. Kirchner, Massachusetts Institute of Technology, August 1976.
15. *Convective Boiling and Condensation*, J. G. Collier and J. H. Thome, Third Edition Oxford Science Publications (1996).
16. Y. Y. Hsu and R. W. Graham, *Transport Processes in Boiling and Two-Phase Systems*, McGraw-Hill, New York, 1976.
17. R. W. Shumway, *TRAC-PF1 Post-CHF Heat Transfer Coefficient Variation for CSAU, Appendix O to Quantifying Reactor Safety Margins: Application of Code Scaling, Applicability, and Uncertainty Evaluation Methodology to a Large-Break, Loss-of-Coolant Accident*, NUREG/CR-5249, EGG-2552, December 1989.
18. G. Th. Analytis, M. Richner, and S. N. Aksan, *Assessment of Interfacial Shear and Wall Heat Transfer of RELAP5/MOD2/36.02 During Reflood*, EIR-Bericht Nr. 624, May 1987.
19. EMF-2102 (P), *S-RELAP5 Verification and Validation*, Framatome ANP, August 2001.
20. "PWR FLECHT-SEASET Unblocked Bundle, Forced And Gravity Reflood Task Data Report," Volume 1 and Volume 2, NUREG/CR-1532, EPRI NP-1459, WCAP-9699, June 1980.

21. "PWR FLECHT Low Flooding Rate Skewed Test Series Data Report," Volume 1 and Volume 2, WCAP-9108, May 1977.

Appendix G Rod-to-Rod Radiation

Thermal radiation effects are present in all heat transfer processes. While the S-RELAP5 code does include thermal radiation models for heat transfer from walls or rods to liquid and vapor, it does not have a wall-to-rod or rod-to-rod thermal radiation heat transfer model. The argument against including this model was that since rod-to-rod temperatures among fuel assemblies in PWRs have relatively small thermal variance, thermal radiation represents only a small fraction of the total heat transfer in a fuel assembly. The challenge to this assertion is that codes like S-RELAP5 are benchmarked, assessed, and tuned against experimental programs that have inherent thermal radiation affects. Given that computer codes like S-RELAP5 generally show good agreement with these tests, the impact of wall-to-rod or rod-to-rod thermal radiations is either truly negligible or is being compensated by other mechanisms

G.1 Qualitative Assessment of Thermal Radiation for Best-Estimate Methodologies

Realistic methodologies, like Framatome ANP's RLBLOCA, have a unique challenge with regard to thermal radiation assessment; that is, there are insufficient data available to isolate and define biases and uncertainties for this specific heat transfer mechanism. In general, this is true for any heat transfer process in which multiple heat transfer mechanisms are present simultaneously. In the DFFB regime, for example, the S-RELAP5 code has models for convective heat transfer to liquid, convection heat transfer to vapor, and thermal radiation heat transfer from the wall to both the liquid and vapor coolant streams. However, the available data only support the determination of a lumped bias and uncertainty for the total heat transfer.

To develop a realistic methodology, assessments must be selected to cover the appropriate range of important phenomena associated with both the event and plant type being analyzed. Covering the appropriate range is necessary to demonstrate that the methodology can adequately treat the event from initiation to conclusion and to prevent the development of an analysis bias. If only high PCT assessments were run, then there would be a potential to exaggerate rod-to-rod radiation effects. This could result in an inappropriate code bias and uncertainty such that the methodology would not correctly predict the heat transfer in the analysis. Consequently, assessments must be selected that demonstrate code applicability over the range of phenomena and allow for the definition of both a bias and uncertainty that is applicable over this range.

Rod-to-rod radiation is important when there is little water present between fuel rods. This is a condition that commonly occurs during dispersed flow film boiling with high void fractions. The experimental programs selected for use to assess and determine the S-RELAP5 code heat transfer bias and uncertainty for this condition were the FLECHT, FLECHT-SEASET and THTF tests as described in Reference 1. As previously indicated, tests were selected from these facilities that covered a range of PCTs for two reasons:

1. To demonstrate that the S-RELAP5 code was capable of predicting PCTs over the appropriate range and at both high and low temperatures.
2. To develop code biases and uncertainties from the code comparison to the measured data over this same range.

The FLECHT and FLECHT-SEASET tests evaluated covered a range of PCTs from 1,651 to 2,239°F and the THTF tests covered a range of PCTs from 1,000 to 2,200°F.

A FANP RLBLOCA methodology development objective was to ensure that rod-to-rod thermal radiation effects were minimized during the derivation of the RLBLOCA heat transfer code uncertainties. This was accomplished by removing test data that could contribute a bias to the final result. This reduced or eliminated scale-effects that might contribute excessive radiant heat transfer from the overall heat transfer model. The FLECHT-SEASET rod data removed from the FANP heat transfer database included those rods identified in Figure 6-4 of WCAP-9891 (Reference 2) as "cold rods." This approach significantly reduced the potential bias on the model resulting from the cold-wall-effect of the assembly housing on radiant heat transfer by shielding the rods of interest from the cold wall with a bank of high power rods.

To demonstrate that this method for selecting and processing the assessments did not result in any bias in the calculated code-to-data bias, three other independent assessments were used to evaluate the calculated code biases. These independent assessments were selected from the CCTF, LOFT, and Semiscale facilities. These three facilities were selected because they were integral type facilities and covered a wide range of scale. Thus, they also served to show that there were no scale effects evident in the code calculations.

The results of these calculations are provided in Section 4.3.4, Evaluation of Code Biases, page 4-100, of Reference 1. The CCTF results are shown in Figures 4.180 through 4.192, the LOFT results in Figures 4.193 through 4.201, and the Semiscale results in Figures 4.202 through 4.207. These figures demonstrate that the comparison between the code calculation and data

is improved with the application of the calculated code biases. This is the expected result since the purpose of the calculated code biases is to improve the code prediction relative to the measured data. The results of these independent calculations indicate that there is no significant impact of not having a rod-to-rod radiation model in the S-RELAP5 code. The measured PCTs in these independent assessments ranged from approximately 1,000 to 1,540°F. At these PCT temperatures, there is little rod-to-rod radiation. Given the good agreement between the biased code calculations and the CCTF, LOFT, and Semiscale data, it can be concluded that there is no significant over prediction of the total heat transfer coefficient due to not having an explicit rod-to-rod radiation heat transfer model in S-RELAP5.

G.2 Supplemental Quantification of the Impact of Thermal Radiation

Additional analyses were performed to demonstrate that calculated radiant heat transfer expected from high temperature 15x15 and 17x17 fuel assemblies exceeds that considered in the S-RELAP5 code assessment and uncertainty analysis applying FLECHT-SEASET data. By neglecting this heat transfer mechanism, clad temperatures predicted by the RLBLOCA methodology are expected to be higher; hence, conservative relative to the acceptance criteria limits.

To estimate the rod-to-rod radiant heat transfer expected within a fuel assembly, FANP applied the R2RRAD thermal rod-to-rod radiation computer code. The theoretical basis for this code is given in References 3 and 4 and is similar to that developed in the HUXY rod heatup code (Reference 5, Section 2.1.2) used by FANP for BWR LOCA applications. The R2RRAD code was developed to examine the rod-to-rod radiation characteristics of 5x5 or smaller rod arrays. When the code was being evaluated for applicability to this particular question, it was concluded that expanding the code capability for the analysis of 6x6 arrays and accounting for the larger guide tube size would provided a better quarter assembly representation. Since a 17x17 FANP Advanced Mark-BW assembly is symmetric on the quarter assembly, it was concluded that analysis on this scale was sufficient.

The output provided by the R2RRAD code includes an estimate of the net radiant heat transfer from each rod in the defined array. Heat transfer uncertainties derived for application in the FANP RLBLOCA methodology were developed on an assembly-average basis; thus, the key measure of interest is the aggregate or mean radiant heat transfer from fuel rods. The maximum net rod-to-rod radiant heat transfer represents a statistical tolerance that may be used

to quantify relative conservatism. The aggregate radiant heat transfer is easily evaluated by averaging the set of fuel rod results. This calculation was added to the R2RRAD code.

G.2.1 17x17 Assembly Study

The studies provided in this section compare results from a RLBLOCA analysis modeling a 17x17 fuel assembly and a set of FLECHT-SEASET tests (Reference 6). Since FLECHT-SEASET Test 31504 closely represents the conditions observed in a typical limiting RLBLOCA calculation, it was selected for illustrating common phenomenological characteristics between the RLBLOCA simulation and the experimental database used to qualify the heat transfer package in S-RELAP5. A cross-section of the 6x6 rod arrays representing a quarter assembly for each configuration is shown in Figure G.1. The shaded rods represent guide tubes. Unlike a 17x17 fuel assembly, the FLECHT-SEASET test assembly design was not symmetric. Three quadrants of the FLECHT-SEASET rod array were designed identically as shown in the right view of Figure G.1. The fourth quadrant is identical to a 17x17 fuel assembly configuration shown in the left view of Figure G.1. It is the left view which is the focus of the analysis presented here. The top-left position corresponds to FLECHT-SEASET assembly array Position 3H and is specified as Rod 1 in the R2RRAD code (R2RRAD numbers read right-to-left, top-to-bottom).

The similarity between a 17x17 fuel assembly and the FLECHT-SEASET test is not a coincidence. FLECHT-SEASET Test 31504 was part of a test series specifically designed to be equivalent to Westinghouse 17x17 fuel assemblies. Table G.1 lists and compares the key geometric parameters describing the assemblies needed to calculate the radiant heat transfer component.

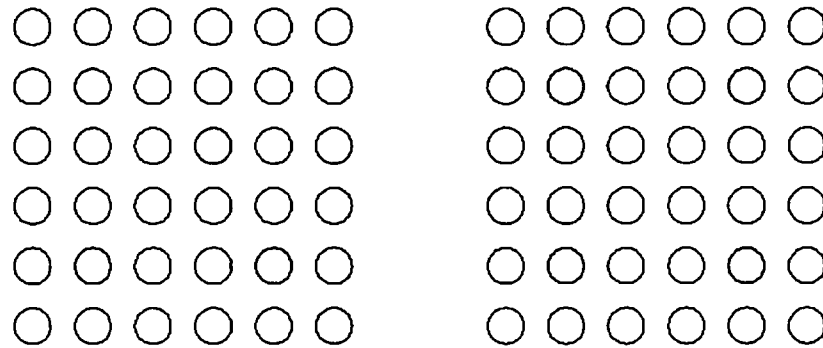


Figure G.1 Quarter Assembly Configurations for the Advanced Mark-BW (left) and the FLECHT-SEASET Tests (right)

Table G.1 Validation Study Design Parameters

Design Parameter	FLECHT-SEASET 31504	17x17 Fuel Assembly
Rod Pitch (in)	0.496	0.496
Fuel Rod Diameter (in)	0.374	0.374
Guide Tube Diameter (in)	0.474	0.482
Guide Tube-to-Fuel Rod Ratio	1.27	1.29
Assembly Hydraulic Diameter (ft)	0.0386	N/A

To compare the FLECHT-SEASET rod assembly to a 17x17 fuel assembly, two analyses using the R2RRAD code were performed to evaluate the thermal radiation as expected in the experiment and the example limiting RLBLOCA analysis, respectively. The first calculation is a direct comparison of the average and maximum rod-to-rod radiation from a limiting RLBLOCA calculation and a FLECHT-SEASET test result having similar temperature characteristics. Since the methodology-defined radial powers set the hot rod to a higher power than the average assembly (which is the realistic configuration), the second analysis captures the effect of a flat power profile across the assembly by setting the hot rod temperature to the hot assembly temperature. The relevant temperature parameters for the first analysis are given in Table G.2. In the RLBLOCA analysis two temperatures can be interpreted as defining the guide tube temperature; the steam temperature or the heat structure temperature. For analysis purposes it is conservative to assume the higher of the two, which is the maximum steam temperature, 1,650°F. This estimate is conservative for comparing to FLECHT-SEASET since the presence

of guide tubes enhances radiant heat transfer; hence, raising the guide tube temperature lowers the thermal rod-to-rod radiation result predicted for the RLBLOCA calculation. In addition, the boundary temperature is evaluated as the average of the surrounding assembly temperature (lower power) and the hot assembly temperature, which coincidentally results in the same value as the guide tube temperature, 1,650°F. The hot rod in all cases was modeled at the position of maximum rod-to-rod radiation as evaluated from the FLECHT-SEASET analysis (i.e., Position 6K or Rod 22 in the R2RRAD code).

Table G.2 Validation Study Design Parameters

Temperature (°F)	RLBLOCA	FLECHT-SEASET 31504
Hot Rod	2,032	2,000
Hot Assembly	1,838	2,000
Guide Tube	1,650	1,750
Boundary	1,650	1,950

The R2RRAD code results for the two analyses are given in Table G.3 ("RLBLOCA (flat)" refers to the analysis considering a flat assembly power profile). At the identified hot rod location (Position 6K) and for the assembly average, the comparison of the FLECHT-SEASET 31504 and the example RLBLOCA calculation results show that the RLBLOCA conditions exhibit more radiation than the FLECHT-SEASET test assembly.

**Table G.3 R2RRAD Code Results: FLECHT-SEASET
Test 31504 versus RLBLOCA Analysis**

Case	Assembly Average HTC (BTU/hr-ft ² -R)	Maximum Rod HTC (BTU/hr-ft ² -R)
RLBLOCA	2.45	9.66
RLBLOCA (flat)	2.41	3.87
31504	1.87	2.62

G.2.2 15x15 Assembly Study

Tests 13609 and 13914 from the FLECHT-Skewed program (Reference 7) were also examined for rod-to-rod radiation in a similar manner as in Test 31504. These cases differ significantly in geometry from Test 31504 in that the rod size is consistent with typical 15x15 fuel array

designs. Table G.4 provides the key geometric parameters needed by the R2RRAD code to describe the fuel assembly. The analysis matrix for this study is provided in Figure G.2.

Table G.4 Tests 13609 and 13914 Design Parameters

Design Parameter	Value
Rod Pitch (in)	0.563
Fuel Rod Diameter (in)	0.422
Guide Tube Diameter (in)	0.545
Guide Tube-to-Fuel rod ratio	1.29

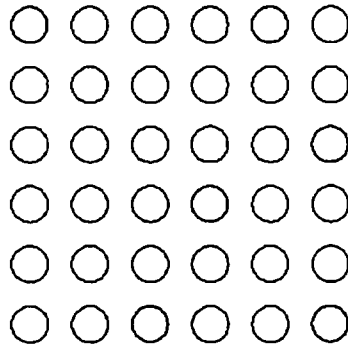


Figure G.2 Quarter Assembly Configurations for Tests 13609 and 13914

The top left corner corresponds to Position 3C as defined in the FLECHT-Skewed test report (Reference 7). In both tests the actual hot rod is one rod position removed from the housing. As stated previously, rod data in this "cold region" was not included in the FANP database. In the region of interest, the hot rod is taken at Position 5E (this corresponds to Rod 15 in the R2RRAD code). The hot rod temperature was taken at the 10-ft location at the time of PCT (from tabulated results given in Reference 7). The guide tube temperature was taken from the steam probe at Position 7C (10-ft location) at the time of PCT for the rod at Position 5E. Due to the limited information in the data report, the hot assembly and boundary temperatures represent averages from the available data channels (rods) in the respective regions at the time of PCT in each data channel. Table G.5 summarizes these calculations (averages rounded to the nearest 25°F). Table G.6 summarizes the key temperature inputs needed for the R2RRAD code and Table G.7 provides the results from those studies.

Table G.5 PCT Temperature for Tests 13609 and 13914 by Position

Position	13609	13914
8B (outside -1)	1,727	1,658
0F (outside)	1,428	1,423
4H	1,749	1,557
5G	1,739	1,660
6E	1,635	1,583
5E	1,748	1,675
Average "Outside" (0F & 8B)	1,575	1,550
Average Rod (4H, 5G, 6E)	1,700	1,600

Table G.6 Key Temperatures for Tests 13609 and 13914

Rod Position	13609	13914
Hot Rod	1,750	1,675
Hot Assembly (Average Rod)	1,700	1,600
Guide Tube	1,450	1,300
"Boundary" Assembly	1,575	1,550

Table G.7 R2RRAD Code Results: Tests 13609 and 13914

Case	Assembly Average HTC (BTU/hr-ft ² -R)	Maximum Rod HTC (BTU/hr-ft ² -R)
RLBLOCA	2.45	9.66
RLBLOCA (flat)	2.41	3.87
13609	2.22	3.55
13914	1.90	3.60

The results from the FLECHT-Skewed test cases show comparable rod-to-rod radiation with respect to the 17x17 configuration. Specifically, the RLBLOCA results bound the test results.

G.2.3 *Minimum Separation of Powers Study*

The purpose of this study was to minimize the difference in temperature between the hot rod and the average rod in the fuel assembly and remove the influence of the guide tubes; thus, minimizing radiation heat transfer. This study proceeds by defining a baseline calculation assuming a 6x6 array of fuel rods in the hot assembly with the following bounding conditions:

- The hot rod is located in Position 16, roughly in the center of the array.
- The hot rod PCT is 2,032°F .
- All remaining rods in the array are at a temperature of 1,975°F.
- The fence (boundary) is at a temperature of 1,975°F.
- No guide tubes were modeled in the array.

This baseline calculation is completed by calculating the minimum equivalent heat transfer coefficient for Rod 16 (near the center of array) and comparing it to the previously presented test data. Using the R2RRAD code, the hot rod radiative heat transfer coefficient is calculated to be 2.6 Btu/hr-ft²-F. This value bounds the test data equivalent heat transfer coefficients of 2.22, 1.90, and 1.87 Btu/hr-ft²-F for the FLECHT and FLECHT-SEASET Tests 13609, 13914, and 31504, respectively. Within the defined problem configuration, the temperature value of 1,975°F for all of the rods surrounding the hot rod represents (by the relationship of temperature to power) a minimum separation of powers between the hot rod and the other hot assembly rods based on the database used to define S-RELAP5 code bias and uncertainty.

Based on the earlier R2RRAD analyses, the use of the actual rod-specific peaking factors for the hot rod and the rods surrounding the hot rod in that example should be expected to result in surrounding rod temperatures lower than 1,975°F (i.e., higher radiation heat transfer). The peaking factors in the example RLBLOCA analysis were a hot rod equal to 1.65 and a hot assembly equal to 1.511. The corresponding temperatures are 2,032 and 1,838 °F (Section G.2.1, Table G.2). An estimate of the minimum separation between the hot rod power and assembly average power can be defined as the radial power measurement uncertainty for the hot rod, typically 4%. This definition of the minimum separation is very conservative relative to what is seen in reactor operation. The average assembly power for a hot rod peaking factor of 1.65 is thus:

$$F_{nom} = \frac{1.65}{1.04} = 1.587 \quad .$$

Interpolating the hot rod and hot assembly temperatures over the power range, the corresponding temperature at the F_{nom} value is:

$$\left(\frac{F_{hr} - F_{nom}}{F_{hr} - F_{ave}} \right) = \left(\frac{T_{hr} - T_{nom}}{T_{hr} - T_{ave}} \right) \Rightarrow \frac{1.65 - 1.587}{1.65 - 1.511} = \frac{2,032 - T_{nom}}{2,032 - 1,838} \Rightarrow T_{nom} = 1,944 \text{ } ^\circ\text{F}.$$

The 1,944 °F temperature defines the maximum average temperature of the remaining fuel assembly rods based on the assumption of minimum separation of powers in the provided example.

With this information, a final R2RRAD calculation was performed examining the minimum separation of powers among the hot rod, hot assembly, and surrounding assemblies for a typical 17x17 fuel assembly. Table G.8 presents the temperature inputs for this problem. Differences from the baseline calculation are that the fence temperature is set to the hot assembly average temperature corresponding to the RLBLOCA hot assembly peaking of 1.511 (representing a bounding minimum separation of power between the surrounding and hot assemblies) and guide tubes are included.

Table G.8 Temperatures for Minimum Separation of Powers Analysis

Temperatures	°F
Hot Rod	2,032
Hot Assembly	1,944
Guide Tube	1,650
Boundary (Fence)	1,838

The minimum hot rod radiant heat transfer is dependent on its location within the assembly. By trial, the limiting location of the hot rod was placed in Rod 11 as shown in Figure G.3 and the guide tube locations are shaded.

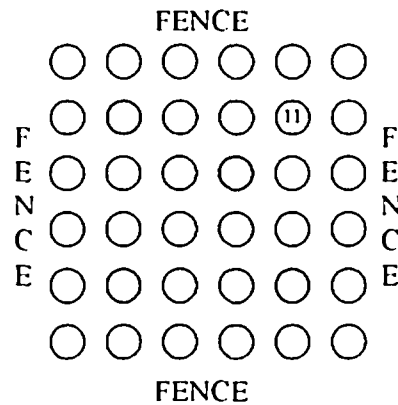


Figure G.3 Location of Rod 11 in the 6x6 Assembly Array

The calculation results are provided in Table G.9. The hot rod radiant heat transfer coefficient is given at Rod 11. Both the assembly average and hot rod results bound the results generated for the FLECHT-SEASET and FLECHT-Skewed studies.

**Table G.9 R2RRAD Code Results: RLBLOCA Analysis
Minimum Radiant Heat Transfer**

Case	Assembly Average HTC (BTU/hr-ft ² -R)	Hot Rod HTC (BTU/hr-ft ² -R)
RLBLOCA (min)	2.5	5.36

The radiation heat transfer coefficient for the generic case, where the separation of power between the hot rod, the hot assembly, and the surrounding assemblies is set conservatively low, remains larger than the radiation heat transfer coefficients calculated from the test data.

G.3 Conclusions

The qualitative assertion that the procedure for evaluating code bias and uncertainty implicitly covers the affect of rod-to-rod thermal radiation was validated by two independent methods. The first method, which was presented as part of the original methodology submittal, demonstrated through confirmatory code assessment calculations (applying the derived code biases) that rod-to-rod thermal radiation was addressed through the derivation of code biases. The second method presented a set of three analyses explicitly showing that estimates of rod-to-rod radiation in the FLECHT-type experiments are bounded by the expected rod-to-rod

radiation that occurs in the reactor. This second set of analyses specifically address the uncertainty associated with radial power and assembly design variations. Based on these results, it can be stated that the RLBLOCA methodology incorporates an inherently conservative treatment of rod-to-rod radiation that does not exaggerate the radiant heat transfer component through application of code bias and uncertainty, and addresses expected power distribution variations within an assembly during plant operation.

G.4 References

1. EMF-2103 (P)(A) Revision 0, *Realistic Large Break LOCA Methodology*, Siemens Power Corporation, April 2003.
2. NUREG/CR-2256, WCAP-9891, "PWR FLECHT SEASET Unblocked Bundle, Forced and Gravity Reflood Task Data Evaluation and Analysis Report," NRC/EPRI/Westinghouse Report No. 10, November 1981.
3. ORNL-5239, "Radiative Heat Transfer in Arrays of Parallel Cylinders," June 1977.
4. D. A. Mandell, "Geometric View Factors for Radiative Heat Transfer within Boiling Water Reactor Fuel Bundles," Nucl. Tech., Vol. 52, March 1981.
5. EMF-CC-130, "HUXY: A Generalized Multirod Heatup Code for BWR Appendix K LOCA Analysis Theory Manual," Framatome ANP, May 2001.
6. NUREG/CR-1532, EPRI NP-1459, WCAP-9699, "PWR FLECHT SEASET Unblocked Bundle, Forced and Gravity Reflood Task Data Report," June 1980.
7. Westinghouse Topical Report WCAP-9108, "FLECHT Low Flooding Rate Skewed Test Series Data Report," dated May 1977.

Appendix H Containment Pressure

The S-RELAP5 code explicitly includes the containment analysis models from Framatome ANP's ICECON containment code (a derivative of the CONTEMPT containment analysis code) for the purpose of providing a best-estimate containment response simulation. This approach is consistent with the NRC's Code Scaling, Applicability, and Uncertainty (CSAU) Methodology (Reference 1). Reference 2 (Sections 3.4.2 and 4.3.3.2.12) briefly describes the calculation of containment pressure and the methodology's treatment of containment pressure by sampling containment volume and temperature. The containment model retains some of the elements of CSB 6-1.

Containment pressure is recognized in the FANP RLBLOCA methodology as a phenomenon of medium to high importance within the Phenomena Identification and Ranking Table (PIRT) context of the CSAU methodology. The PIRT outcome yielded two important containment parameters – containment volume and temperature, representing the only quantifiable phenomenological dependency associated with air pressure. The heat transfer to passive heat sinks is treated as best-estimate. Containment pressure is influenced by engineered systems such as building sprays, fan coolers, and ice condensers and their treatment is based on component-specific performance expectations.

H.1 S-RELAP5 Containment Model History

The NRC review and approval history for the containment models used in S-RELAP5 and the RLBLOCA methodology is as follows:

- The SER for Exxon Nuclear Company (ENC) ECCS Evaluation Model (Reference 3) documents NRC review and acceptance for use of CONTEMPT22-ENC (based on Reference 4) in dry containments, including sub-atmospheric containments.
- The SER for the ICECON code (Reference 5) dated June 30, 1978 documents NRC's review and acceptance of ICECON, modified from CONTEMPT22-ENC by adding routines to analyze ice condenser containments. The approved features for analysis of dry containments were retained in ICECON, so that ICECON could be used for analysis of either dry or ice condenser containments.
- The SER for the RLBLOCA topical report, EMF-2103 (Reference 2), documents NRC's review and acceptance of S-RELAP, including its ICECON-based containment module, for the analysis of realistic LBLOCA transients. Containment modeling within a RLBLOCA analysis is as specified in EMF-2103.

The report EMF-CC-039(P) Revision 2 Supplement 1 (Reference 6) provides a description of the input for the ICECON routines used in S-RELAP5 for RLBLOCA analyses. This report was provided to the NRC in the letter NRC:01:037 dated August 21, 2001. The report is Reference 20 in the NRC SER for the topical report EMF-2103 (P).

The ICECON modules incorporated into S-RELAP5 are identical to those in the ICECON code except for the replacement of the Tagami correlation with the Uchida correlation and the changes necessary to interface the modules with S-RELAP5. The implementation of the ICECON code into S-RELAP5 is described in Section 3.4.2 of Reference 2 on pages 3-15 and 3-16.

The ICECON routines are used in S-RELAP5 for the RLBLOCA methodology to provide a realistic containment pressure. A "minimum" containment pressure is not a goal of a realistic calculation. The containment modeling in the RLBLOCA methodology includes both the statistical and non-statistical treatment of significant model inputs. The objective is to obtain containment pressure results that reflect expected containment behavior, including input parameter uncertainties. The dominant phenomenological influences (ignoring active systems) on containment pressure are: heat transfer to internal structures, break size and effluent modeling, and initial pressure. Consistent with the CSAU methodology, the parameters with little influence on containment pressure are modeled by assuming nominal or, in some instances, conservatively-biased values. The net effect of treating certain parameters with conservatively-biased values and other parameters in a statistical manner is to produce a conservatively biased (low) pressure result.

H.2 Containment Model Characterization

The RLBLOCA methodology defines a generic approach to containment modeling. The plant-to-plant variations are accommodated for in this approach. For RLBLOCA analyses the containment pressure is essentially a boundary condition. It may be necessary to incorporate conservative biases to accommodate incomplete plant data. In the extreme case the containment pressure response may be derived from a CSB 6-1 minimum containment pressure calculation. At a minimum, a utility customer has sufficient information to support development of a containment input model consistent with previous licensed modeling efforts, generally an Appendix K evaluation model.

An objective of the CSAU process is to focus on the dominant contributors influencing the measure of interest (i.e., clad temperature). The original LBLOCA PIRT presented in Reference 1 ranked the importance of containment pressure low. For the RLBLOCA methodology, Framatome ANP assigned containment pressure a medium to high importance to acknowledge the affects of steam density and heat transfer (including the steam binding affect on reflood rates and reduced subcooling).

The Framatome ANP RLBLOCA methodology specifically addresses uncertainty associated with containment pressure. Framatome ANP has identified the dominant influences on containment pressure as heat transfer to structures, break size and effluent modeling, and initial pressure (i.e., air mass).

H.2.1 *Passive Heat Sinks – Uchida Model*

The containment response in the RLBLOCA analyses is simulated in S-RELAP5 using the NRC-approved ICECON containment response model with the exception that the Uchida heat transfer correlation with a multiplier of 1.7 is used to model heat transfer to passive containment structures for the entire simulation. The 1.7 multiplier was empirically derived for a dry containment plant. The analysis was performed to equate the heat transfer to containment internals as predicted by the usual Tagami and Uchida model without the CSB 6-1 conservative multipliers to an Uchida-only model. The 1.7 multiplier is validated, or modified, for a plant-specific RLBLOCA application using the procedure described below.

The Uchida model, without augmentation, is presented in References 7 and 8 as being best estimate. The Uchida correlation (without the 1.7 multiplier recommended in the FANP RLBLOCA methodology) was validated in Reference 7. It was concluded that the Uchida correlation provides a best-estimate result when the bulk gas pressure is one atmosphere and that it progressively under predicts pressure at lower bulk gas pressures. The bulk gas pressure is related to the partial pressure of the gas; hence, it remains essentially constant during LOCA (neglecting temperature effects and accumulator nitrogen). It follows that applying Uchida with a 1.7 multiplier would be conservative for current generation wet and dry PWR containment designs. Uchida's acceptability was also demonstrated via comparisons to GOTHIC predictions. In addition, developmental assessment of GOTHIC has presented the Uchida model (without augmentation) as being a best-estimate model (see Reference 8).

Containment models for RLBLOCA analyses are developed following a process consistent with the approved methodology and a typical RLBLOCA analysis. To establish model confidence, the FANP RLBLOCA guidelines require a benchmark against a best-estimate containment analysis or minimum containment pressure calculation. Figure H.1 presents the result from a typical assessment. In the event that the S-RELAP5 model significantly over predicts system pressure (> 1 psi after blowdown), the Uchida multiplier is used to tune the containment pressure response to the benchmark.

Figure H.2 shows the containment pressure range (case-independent) from a typical RLBLOCA analysis, a FSAR (Appendix K-type) minimum containment pressure prediction, and the containment pressure from the calculation reporting the limiting PCT. This comparison indicates that the containment conditions, modeled in accordance with FANP RLBLOCA methodology, encompass a wide range of conditions. Figure H.2 also indicates that the containment pressure predicted from the RLBLOCA calculation encompasses a large part of the predicted Appendix K behavior. This is not a requirement of the methodology, since many unrealistic parameters define the minimum containment pressure calculation.

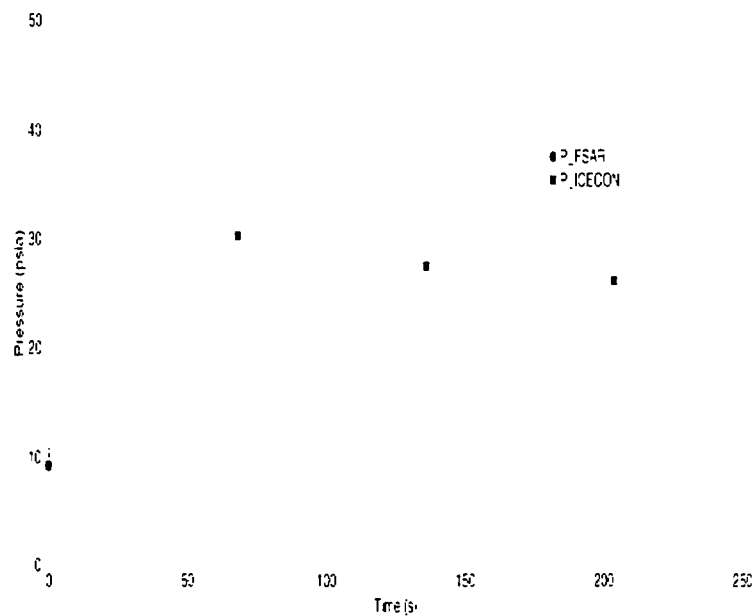


Figure H.1 Example Minimum Containment Pressure Benchmark

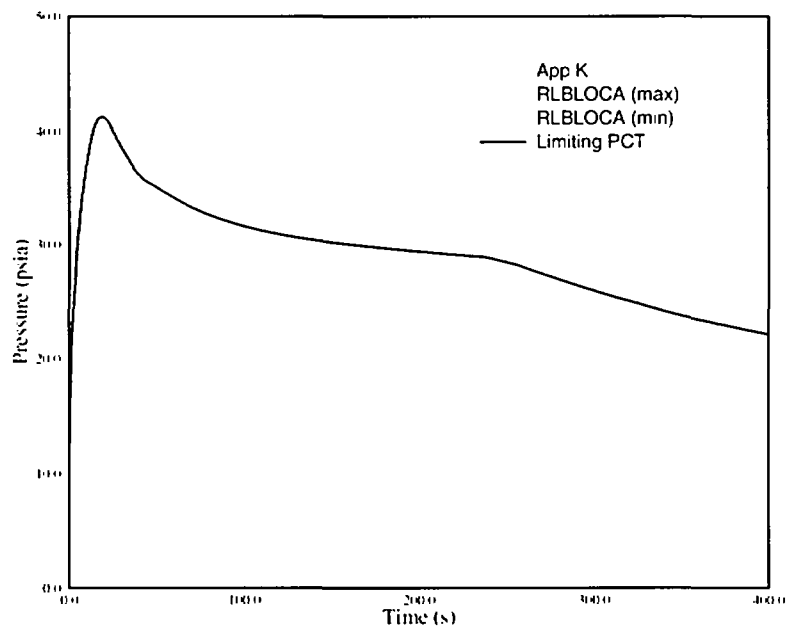


Figure H.2 RLBLOCA Analysis Containment Pressure Range versus Appendix K Result

H.2.2 *Break Flow*

Break flow was shown to be the dominant influence on containment pressure. The FANP RLBLOCA methodology statistically ranges break size over the full spectrum of break sizes defined as large breaks. This includes both double-ended and split breaks. Since each unique S-RELAP5 break case is explicitly analyzed for its containment pressure response, the influence of break size contributes to uncertainty in the containment response. The modeling of critical break flow is treated by applying appropriate uncertainties as described in Reference 2.

H.2.3 *Initial Containment Pressure and Temperature*

Since the choke flow condition prevents communication from the containment to the plant reactor coolant system (RCS), initial containment pressure is not in itself an important LBLOCA phenomenon. The initial containment pressure does define the air mass during the LBLOCA simulation. In addition, most plants employ active systems designed to target a desired containment pressure; hence, the uncertainty associated with the initial containment pressure is small. The initial containment pressure is set to a representative value within the allowable Technical Specification range.

The normal variation in initial air mass is accommodated in the RLBLOCA analysis by ranging the containment volume and temperature. The containment volume is sampled for drywell containments between the nominal volume and the "empty volume." The "empty volume" is defined as simply the volume of the containment dome plus the volume of the containment cylinder. This sample range is conservative since the larger containment volume results in lower containment pressures following LOCA initiation. The containment temperature is ranged from a best-estimate minimum to the high containment temperature Technical Specification value. The containment volume and pressure sampling for ice condenser plants is different and described in Section H.2.6.

H.2.4 *Inherent Conservatisms*

The FANP RLBLOCA methodology incorporates a number of conservatisms related to containment modeling:

1. mass and energy are treated in equilibrium by S-RELAP5

2. The modeling of the containment spray systems conservatively takes no credit for single active failures (i.e., full spray is used regardless of assumed single active failure affecting ECCS)
3. the humidity is assumed to be 100 percent

Item one is most important following blowdown when the break flow unchokes and when the ECCS injection represents the majority of the break flow. ECCS injection is modeled in a manner consistent with realistic expectation: all ECCS fluid is injected into the NSSS. The reactor coolant system resistance network determines the amount of ECCS fluid that is discharged into the containment through the break. In the cold leg—including the broken cold leg—the ECCS fluid mixes with steam flow in the RCS. In the broken cold leg, the steam and liquid are then discharged out the break to the containment atmosphere. S-RELAP5 applies the break flow, both steam and liquid components, directly to the containment atmosphere, which is modeled to achieve instantaneous equilibrium. Because of this treatment, there is no effective difference between modeling the mixing to occur in the cold leg prior to discharge from the break and modeling the mixing of the steam and liquid flows separately in the containment atmosphere. The degree to which the ECCS is heated in the mixing process in the cold leg is counterbalanced by de-superheating of the steam flow. If the ECCS fluid were modeled as direct spillage, a realistic treatment would represent spillage to the containment floor versus the clearly conservative instant equilibrium in the containment atmosphere assumed in the RLBLOCA model, which effectively treats the ECCS fluid as an additional containment spray.

Item two relates to the choice of the worst single active failure sampled in a RLBLOCA calculation. The containment pressure uncertainty associated with the assumed worst single failure is treated by applying full spray regardless of the sampled worst single failure. The RLBLOCA methodology samples the worst single failure as either a loss of one diesel generator or the loss of one low pressure safety injection pump. Full spray would not be available for a loss of diesel generator; however, the RLBLOCA methodology conservatively ignores this condition.

Item 3 relates to the fact that minimizing air mass is conservative; hence, consistent with CSB 6-1, the RLBLOCA methodology conservatively assumes 100 percent humidity within the containment vessel. Total air mass is calculated as a function of initial pressure, temperature and humidity.

H.2.5 *Choice of Nominal Versus Conservative Values*

The Branch Technical Position CSB 6-1 was established to provide guidance to plant licensees and vendors regarding containment systems modeling for Appendix K-based LOCA evaluations. The intent of CSB 6-1 is to provide guidance for the performance of a "minimum" containment backpressure analysis. The FANP RLBLOCA methodology was approved as a realistic methodology that conforms to Regulatory Guide 1.157. Regarding containment pressure, the Regulatory Guide states (Section 3.12.1):

"The containment pressure used for evaluating cooling effectiveness during the post-blowdown phase of a loss-of-coolant accident should be calculated in a best-estimate manner and should include the effects of operation of all pressure-reducing equipment assumed to be available. Best-estimate models will be considered acceptable provided their technical basis is demonstrated with appropriate data and analyses."

The containment pressure response used in RLBLOCA analyses is a result of applying both best-estimate and conservative modeling assumptions. The CSAU methodology requires that the treatment of important phenomena accommodate anticipated uncertainties and considers that this is sufficient to express the total uncertainty measures with a "high probability that acceptance criteria are not exceeded" (Regulatory Guide 1.157).

As previously stated, the dominant phenomena influencing containment response are: heat transfer to internal structures, break size and effluent modeling, and initial pressure. Parameters with a lesser phenomenological influence may be modeled nominal or biased (e.g., applying CSB 6-1 recommendations). Plant data must be available to define the nominal values used. For example, performance specifications that relate to containment modeling parameters do not necessarily reflect realistic performance expectations. Spray pump performance, for instance, is affected by form and flow restrictions that physically prevent spray systems from operating at maximum rated flow conditions. Plant data are used in this situation to differentiate ideal and best-estimate performance expectations. Using conservative performance specifications (per CSB 6-1) is appropriate when the nominal information is unavailable.

Regulatory Guide 1.157 states that best-estimate models may be used for containment pressure simulation, provided they can be supported by data and analysis. This statement contrasts to the statement in Section 3.1 of the Regulatory Guide 1.157 that states "Other boundary and initial conditions and equipment availability should be based on plant technical

specification limits." With regard to Technical Specifications addressed for containment modeling, the FANP RLBLOCA methodology is consistent with the first statement. If through data or system analysis, it can be shown that a particular plant Technical Specification has little influence on containment pressure, it is then unnecessary to use the LBLOCA scenario in support of the Technical Specification. For example, reserve water storage tank (RWST) temperature is typically defined with both a high and low Technical Specification value. For LBLOCA analysis, RWST temperature primarily contributes to clad temperature by defining the liquid subcooling of the LPSI coolant. A secondary influence is the cooling affect on containment spray. Figure H.3 shows an analysis comparing the containment pressure result from calculations assuming a nominal value versus the Technical Specification low value. The result shows that its influence is negligible over the design range; hence, the explicit treatment of this Technical Specification is unnecessary. The service water temperature is treated in the same manner.

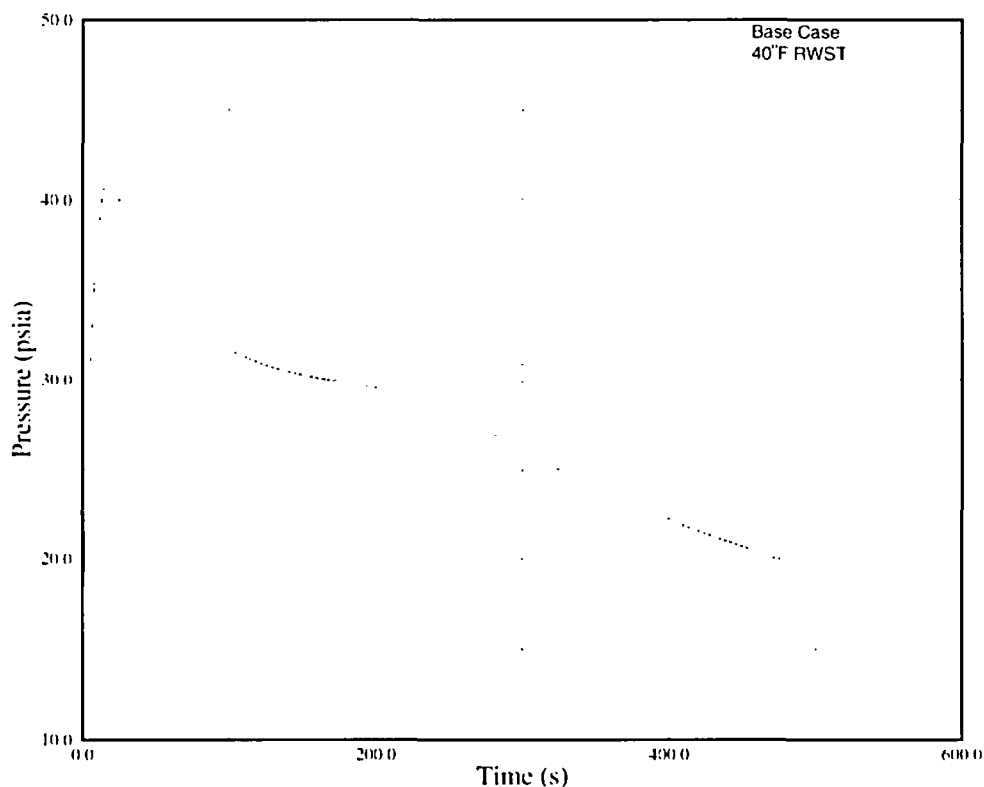


Figure H.3 Containment Pressure Sensitivity to RWST Temperatures of 40 and 45°F

Table H.1 provides a comparison of key model inputs, as identified in Branch Technical Position CSB 6-1, to the treatment of these items in the FANP RLBLOCA guidelines. Inspection of the tabulated model parameters illustrates the method as well as the degree of conservatism for the containment pressure response.

Table H.1 Comparison of CSB 6-1 Model Parameters to RLBLOCA Analysis

Model Parameter	CSB 6-1	FANP RLBLOCA
Initial Containment Internal Condition		
Containment Gas Temperature	MIN (drywell) MAX (ice)	Sampled
Containment Pressure	Minimum	Nominal
Humidity ^a	100%	100%
Initial Outside Containment Ambient Conditions		
Temperature ^a	"reasonably low"	N/A ^b
Containment Volume	MAX free volume	Sampled (nominal to maximum volume)
Purge Supply and Exhaust Systems	Open purge lines	N/A ^c
Active Heat Sinks		
Spray Flow	MAX	Nominal ^d or Bounding (high)
Spray Temperature	MIN	Nominal ^d or Bounding (low)
Fan Cooler Heat Removal	MAX	Nominal ^d or Bounding (high)
Containment Steam Mixing with Spilled ECCS Water	"should be considered"	Approved Code Model Applied
Containment Steam Mixing with Water from Ice Melt	"should be considered"	Approved Code Model Applied
Passive Heat Sinks	"structures... influence[ing] containment pressure"	Included
Heat Transfer Coefficients	4 x Tagami (blowdown) and 1.2 x Uchida (refill/reflood)	1.7 x Uchida (Section H.2.1)

^a Containment pressure simulations do not show significant sensitivity to this parameter.

^b For short transients like LBLOCA, heat transfer to the environment outside of the containment is negligible.

^c Included in total volume, if necessary.

^d Nominal, if sufficient justification can be developed. Spray and fan cooler system efficiencies are treated in a similar manner.

H.2.6 *Drywell Versus Ice Condenser Containment Modeling and Uncertainty Treatment*

The two common PWR containment designs are drywell and ice condenser. The basic drywell containment is represented by a single compartment volume. Atmospheric conditions in this compartment respond to the mass and energy calculated from the simulated break and the engineered cooling systems. The ice condenser containment is modeled by an ice condenser and three compartments volumes: deadend, lower, and upper. The reactor coolant system of a plant is attached to the lower compartment which is directly coupled with the deadend compartment. Communication with the upper compartment occurs when there is a pressure imbalance between the lower and upper compartments which forces flow through the ice condenser or when deck fans actuate forcing flow between the compartments.

Compartment modeling is consistent regardless of containment type. Each compartment is described by volume, pressure, temperature, surface area, etc. and passive heat sinks can be attached. The ice condenser model input requires a detailed structural description which is based on plant-specific design specifications including ice mass, surface area, and ice bay flow area.

The air mass is the primary uncertainty treated with the containment model. The treatment of air mass in drywell containments is described in Section H.2.3. The sampling of containment air mass is handled in a manner appropriate to the nature of ice condenser containments. The ice condenser plays a special role in removing energy from the atmosphere. The plant air mass is important; however, the initial location of air mass is also important. This is because there is uncertainty associated with how much atmosphere from the lower compartment arrives in the upper compartment. To maximize the amount of atmosphere that moves through the ice condenser, the deadend and lower compartment volumes are biased to a net minimum value. The upper compartment volume is ranged from a net minimum value to the gross total containment volume minus the net minimum volumes of the lower compartment and deadend volumes minus gross ice condenser volume. The sampling of the lower and upper compartment temperatures are also different from that prescribed for drywell plants. They are sampled over separately specified temperature ranges; however, the sampling is correlated by using the same random number in the sampling process.

The dynamics of ice melt is an intrinsic feature of the containment models used in S-RELAP5 (inherited from the ICECON code). Ice melt is introduced to the containment like a spray.

References 5 and 6 provide a detailed description of the previously approved ice condenser model.

H.3 Impact of Unmodeled Parameters

The CSAU methodology recognizes a threshold of the importance for parameters describing a system of interest. This section addresses the question: what is the impact of any unmodeled plant or phenomenological characteristic? This includes situations such as plant operational changes or a modeling oversight. A sensitivity study, based on a deterministic perturbation to the base result, can be performed to estimate the impact of not specifically modeling a particular uncertainty.

The general method to estimate the impact on the 95/95 total uncertainty statement from a perturbation of any “unmodeled” uncertainty follows from the condition that the 95/95 total uncertainty statement reflects the combination of each individual uncertainty component. From statistics, the total uncertainty for a set of mutually uncorrelated random variables is (as used in the Framatome ANP RLBLOCA methodology)

$$\sigma_x^2 = \sum_{i=1}^n \sigma_i^2 \quad ,$$

where σ_x is the total uncertainty from a set of individual uncertainty contributors, σ_i . While the usual statement of uncertainty is the standard deviation, the prior equation is valid for any statement of uncertainty, such as the 95/95 limit. For example, assuming that the total uncertainty associated with the LBLOCA problem (difference between the 95/95 PCT and the 50/50 PCT), σ_x , is 437°F, a bounding estimate of σ_i for a particular unmodeled parameter can be found by performing a deterministic sensitivity study at the anticipated parameter limit. If in this example the result of the deterministic calculation shows a variance of 30°F, the estimated impact on the 95/95 limit is calculated from

$$\left(\sigma_x^2 + \sigma_{n+1}^2\right)^{\frac{1}{2}} - \sigma_x = \left(437^2 + 30^2\right)^{\frac{1}{2}} - 437 \approx 1^\circ\text{F}$$

In this example, the maximum impact on the total uncertainty statement is 1°F. It is expected that the uncertainty effects from parameters for which the uncertainties are not modeled will both increase and decrease clad temperatures, negating any impact on the total uncertainty.

H.4 Conclusion

In summary, Framatome ANP's RLBLOCA methodology for the calculation of containment pressure is qualified as a best-estimate calculation consistent with Regulatory Guide 1.157. The modeling approach produces a distribution of containment pressure responses through ranging of containment volume and temperature. This distribution of containment pressures is sufficiently broad to encompass the effects of model uncertainties and biases. The overall approach to calculate containment pressure is more realistic than an Appendix K approach but is biased in the conservative direction.

H.5 References

1. Technical Program Group, "Quantifying Reactor Safety Margins: Application of Code Scaling, Applicability, and Uncertainty Evaluation Methodology to a Large Break Loss of Coolant Accident," EG&G Idaho, Inc., NUREG/CR-5249, December 1989.
2. EMF-2103(P)(A) Revision 0, *Realistic Large Break LOCA Methodology for Pressurized Water Reactors*, Framatome ANP, April 2003.
3. XN-75-41, *ENC WREM-Based Generic PWR ECCS Evaluation Model*, Exxon Nuclear Company, July 1975.
4. Wheat, Larry L. , *CONTEMPT-LT A Computer Program for Predicting Containment Pressure-Temperature Response to a Loss-Of-Coolant-Accident*, Aerojet Nuclear Company, TID-4500, ANCR-1219, June 1975.
5. XN-CC-39(A), *ICECON A Computer Program Used to Calculate Containment Back Pressure for LOCA Analysis (Including Ice Condenser Plants)*, Exxon Nuclear Company, October 1978.
6. EMF-CC-39 (P), *ICECON A Computer Program Used to Calculate Containment Back Pressure for LOCA Analysis (Including Ice Condenser Plants)*, Siemens Power Corporation, December 1999.
7. P. F. Peterson, "Theoretical basis for the Uchida correlation for condensation in reactor containments," *Nuclear Engineering and Design*, 162 (1996), pg 301-306.
8. T. L. George, et al., "GOTHIC Containment Analysis Package Qualification Report," NAI 8907-09 Revision 5, Richland, Washington, July 1999.

Appendix I Downcomer Heat Structure Nodalization Technical Basis

Heat structure nodalization of the reactor vessel downcomer modeled for RLBLOCA analyses applies a progressive noding scheme. This nodalization scheme is the result of sensitivity studies performed to address the generalized problem of numerical heat conduction. There are no universal rules about nodalization schemes for heat conduction; however, the accuracy of numerical heat conduction simulations is dependent on time step and mesh spacing – but, time steps used in S-RELAP5 are based on processes with faster response times than heat conduction.

The sensitivity studies performed for mesh spacing have validated the assertion that mesh spacing near the heat conductor's surface based on a Biot number of 1.0 is sufficient for all phases of a large break LOCA. The Biot number is expressed as

$$Bi = \frac{h\Delta x}{k},$$

where Δx is the mesh spacing, h is the heat transfer coefficient and k is the thermal conductivity. For common reactor vessel materials exposed to post-blowdown environment, this assumption results in a surface mesh size less than 0.025 ft. (Note: during blowdown, conduction from passive heat structures is conduction limited; that is, conduction is unaffected by changes in fluid convection.) The progressive mesh spacing scheme of doubling mesh sizes was evaluated by sensitivity studies and demonstrated to be as accurate as using uniform mesh spacing equivalent to the surface mesh spacing size. The heat structure nodalization used for all passive heat conductors in RLBLOCA analyses, including the downcomer, apply a mesh spacing finer than those evaluated through sensitivity studies. It follows that the simulation of heat removal from the downcomer represents an accurate and best-estimate simulation of the heat conduction process.

Attachment B

**Change Pages for EMF-2103, "Realistic Large Break LOCA Methodology
for Pressurized Water Reactors"**

Non-Proprietary

summary is provided giving the parameter bias and uncertainty and how it is to be applied in the methodology. In addition to these parameters, a few other parameters are being treated statistically based on analysis other than code assessment. The discussion on these parameters includes additional background and explanation of the objective of the statistical treatment. Table 4.19 presents a summary of the key statistical characteristics used in the FRA-ANP RLBLOCA methodology. The table provides a list of biases, standard deviations (for parameters treated with a normal probability distribution function), and range boundaries ($\pm 2\sigma$ for normal probability distribution functions).

4.3.3.2.1 Stored Energy

The analysis of stored energy uncertainty was performed by assessing RODEX3A predictions for centerline fuel temperature relative to data taken at the Halden Reactor Project. The results are presented in Section 5.8 of Reference 5. Using a normal probability distribution function, the mean error in centerline fuel temperature is 0.0 with a standard deviation of 130 °F. A bias in centerline temperature has been identified for burnup greater than 10 MWd/kgU. This is given by the expression:

$$Y(^{\circ}\text{F}) = -4.2232 * X(\text{MWd/kgU}) + 39.183 ^{\circ}\text{F}$$

The parameter is first sampled using a normal distribution with a mean of 0.0 and standard deviation of 130 °F. A test on "Time-of-Cycle" is performed to check if the bias is to be applied. If so, the bias is combined with the sampled centerline fuel temperature. In applying the sampled fuel centerline temperature, the S-RELAP5 multiplier, FUELK, is used in conjunction with a control system that tracks the centerline temperature of the peak power node. The FUELK multiplier is applied to the fuel pellet thermal conductivity. Using a control system applied during a steady-state S-RELAP5 calculation, this multiplier is driven to a value that results in shifting the fuel centerline temperature from a best-estimate value to the best-estimate value plus uncertainties as given by the equation above.

4.3.3.2.2 Oxidation

Energy released through the oxidation of cladding is calculated from the Cathcart-Pawel correlation (Reference 25) for oxide layer growth:

Table 4.19 Summary of Evaluated Uncertainties of key PIRT Parameters



-]
1. [
 -]
 2. [
 -]
 3. [
 -]
 4. [
 -]
 5. [
 -]

The data produced by this method is used primarily to develop input for the RODEX3A code.

[

]

5.1.3.3 Treatment of Axial and Radial Power Shapes

To support a plant's technical specification for the core peaking factor, F_q , the axial power shape must be adjusted from the nominal axial power shape extracted for the limiting fuel rod. During normal operation, F_q will most likely occur relatively near the nominal F_q represented in the power history files. [

]

- []
- []
- []
- []
- []
- []
- []
- []

5.1.4 Supporting Ranges Without Data

As shown in Table 5.1, some parameters lack explicit definition (technical specifications or data). For parameters for which no plant data is available, ranges may be established based on physical constraints or by analytical methods. Examples of physical limits include ranging the vessel upper head temperature to a maximum value of the hot leg temperature or ranging the diesel start delay on the LPSI pumps to a time corresponding to when RCS pressure drops below the back pressure delivered by the LPSI pumps. It may also be demonstrated that a particular parameter has a limited range of influence based on a set of sensitivity studies.

5.1.5 Reporting of Treatment of Process Parameters

Many decisions are required to establish plant specific treatment of process parameters. Such decisions must be reported or referenced when issuing a safety analysis report. Because the ranges and statistical description of the behavior of plant parameters may vary from plant to plant, the safety analysis report will require an explicit discussion of the treatment of key process parameters. If no changes are made in the treatment of process parameters for subsequent analyses, the earlier report may be referenced.

5.2 *Performance of NPP Sensitivity Calculations (CSAU Step 12)*

5.2.1 Statistical Approach

[

Attachment B

Change Pages for EMF-2103, "Realistic Large Break LOCA Methodology
for Pressurized Water Reactors"

Non-Proprietary

summary is provided giving the parameter bias and uncertainty and how it is to be applied in the methodology. In addition to these parameters, a few other parameters are being treated statistically based on analysis other than code assessment. The discussion on these parameters includes additional background and explanation of the objective of the statistical treatment. Table 4.19 presents a summary of the key statistical characteristics used in the FRA-ANP RLBLOCA methodology. The table provides a list of biases, standard deviations (for parameters treated with a normal probability distribution function), and range boundaries ($\pm 2\sigma$ for normal probability distribution functions).

4.3.3.2.1 Stored Energy

The analysis of stored energy uncertainty was performed by assessing RODEX3A predictions for centerline fuel temperature relative to data taken at the Halden Reactor Project. The results are presented in Section 5.8 of Reference 5. Using a normal probability distribution function, the mean error in centerline fuel temperature is 0.0 with a standard deviation of 130 °F. A bias in centerline temperature has been identified for burnup greater than 10 MWd/kgU. This is given by the expression:

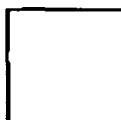
$$Y(^{\circ}\text{F}) = -4.2232 * X(\text{MWd/kgU}) + 39.183 ^{\circ}\text{F}$$

The parameter is first sampled using a normal distribution with a mean of 0.0 and standard deviation of 130 °F. A test on "Time-of-Cycle" is performed to check if the bias is to be applied. If so, the bias is combined with the sampled centerline fuel temperature. In applying the sampled fuel centerline temperature, the S-RELAP5 multiplier, FUELK, is used in conjunction with a control system that tracks the centerline temperature of the peak power node. The FUELK multiplier is applied to the fuel pellet thermal conductivity. Using a control system applied during a steady-state S-RELAP5 calculation, this multiplier is driven to a value that results in shifting the fuel centerline temperature from a best-estimate value to the best-estimate value plus uncertainties as given by the equation above.

4.3.3.2.2 Oxidation

Energy released through the oxidation of cladding is calculated from the Cathcart-Pawel correlation (Reference 25) for oxide layer growth:

Table 4.19 Summary of Evaluated Uncertainties of key PIRT Parameters



1.]
2. []
3. []
4. []
5. []

The data produced by this method is used primarily to develop input for the RODEX3A code.

[]

5.1.3.3 Treatment of Axial and Radial Power Shapes

To support a plant's technical specification for the core peaking factor, F_q , the axial power shape must be adjusted from the nominal axial power shape extracted for the limiting fuel rod. During normal operation, F_q will most likely occur relatively near the nominal F_q represented in the power history files. []

]

- []
- []
- []
- []
- []
- []
- []
- []

5.1.4 Supporting Ranges Without Data

As shown in Table 5.1, some parameters lack explicit definition (technical specifications or data). For parameters for which no plant data is available, ranges may be established based on physical constraints or by analytical methods. Examples of physical limits include ranging the vessel upper head temperature to a maximum value of the hot leg temperature or ranging the diesel start delay on the LPSI pumps to a time corresponding to when RCS pressure drops below the back pressure delivered by the LPSI pumps. It may also be demonstrated that a particular parameter has a limited range of influence based on a set of sensitivity studies.

5.1.5 Reporting of Treatment of Process Parameters

Many decisions are required to establish plant specific treatment of process parameters. Such decisions must be reported or referenced when issuing a safety analysis report. Because the ranges and statistical description of the behavior of plant parameters may vary from plant to plant, the safety analysis report will require an explicit discussion of the treatment of key process parameters. If no changes are made in the treatment of process parameters for subsequent analyses, the earlier report may be referenced.

5.2 Performance of NPP Sensitivity Calculations (CSAU Step 12)

5.2.1 Statistical Approach

[